

---

# Age of the basement beneath the Mesozoic Lusitanian Basin revealed by granitic xenoliths from the Papôa volcanic breccia (West Iberia)

---

M.F. Pereira<sup>1</sup> C. Gama<sup>1</sup> J.B. Silva<sup>2</sup> Í. Dias da Silva<sup>3</sup>

<sup>1</sup>Instituto de Ciências da Terra, Departamento de Geociências, ECT, Universidade de Évora  
Apt. 94, 7002-554 Évora, Portugal. Pereira E-mail: mpereira@uevora.pt

<sup>2</sup>Instituto Dom Luiz, Departamento de Geologia, Faculdade de Ciências da Universidade de Lisboa  
Campo Grande, 1749-016 Lisboa, Portugal

<sup>3</sup>Instituto Dom Luiz, Faculdade de Ciências da Universidade de Lisboa  
Campo Grande, 1749-016 Lisboa, Portugal

---

## | A B S T R A C T |

---

The dyke of the Papôa volcanic breccia cross-cutting the Lower Jurassic sequence of the Lusitanian Basin (West Iberia) contains granitic xenoliths. In this study, for the first time, U-Th-Pb zircon analysis of two xenoliths yielded c. 298Ma for the biotite granite and of c. 305-291Ma for the two-mica granite, indicating that the pre-Mesozoic basement of the Lusitanian Basin includes Permian intrusions. These ages are close within the margin of error to the age of the Late Carboniferous granites of the Berlengas isles that with the Late Devonian high-grade metamorphic rocks of the Farilhões isles, located northwest of the study area, form the pre-Mesozoic basement of the Lusitanian Basin. These new geochronological findings enable us to establish that Permo-Carboniferous magmatism lasted at least 14Ma in this region, as in other regions of the Appalachian-Variscan belt. Furthermore, a comparison with available data from Paleozoic tectonic units of the Appalachian-Variscan belt located in and outside the Iberian Massif suggests that the Lusitanian Basin (Peniche) most probably rests on the South Portuguese Zone, which may correlates with the Rhenohercynian Zone present in southwest England, and the Meguma terrane of Nova Scotia.

---

**KEYWORDS** | Pyroclastic breccia. Xenoliths. Granitic rocks. U-Pb zircon dating.

## INTRODUCTION

The study of xenoliths in volcanic pipes can enable the characterization of the magmatic and metamorphic rocks that constitute the crust at depth. This approach is particularly relevant where such rocks that have formed at deeper crustal levels are not exposed in a given basin or occur hundreds of kilometres away from the basin with no apparent relationship with it. The ascent of magma to its level of extrusion may involve the incorporation

of fragments of solid rock material from the host rocks through which it has passed (e.g. [Dostal et al., 2005](#); [Puelles et al., 2019](#)). Therefore, a volcanic pipe that cuts a sedimentary basin, whose basement rocks are unknown, may provide evidence of the deeper crustal rocks preserved as xenoliths, of which granites are a good example. This paper describes the field occurrence of two granitic xenoliths from the Papôa intrusive volcanic breccia in the Jurassic strata of the Lusitanian Basin (western Iberia).

In the present study, for the first time, zircon grains extracted from xenoliths of granite from a post-Sinemurian volcanic breccia are described using cathodoluminescence imaging and SHRIMP U-Pb geochronology. The findings are compared with the available literature and used to discuss the pre-Mesozoic basement of the Lusitanian Basin. We have considered not only the Paleozoic tectonic units from the Iberian Massif but also those located in other parts of the Appalachian-Variscan belt, such as Nova Scotia and southwest England. The analysis of the composition and age of the breccia matrix and other type of xenoliths are beyond the objective of the present study.

## GEOLOGICAL SETTING

### Lusitanian Basin

In western Iberia, the Mesozoic Lusitanian Basin extends landwards for about 250 kilometres along the coastline of Portugal from Setúbal to Porto (Fig. 1). In the Peniche region, a well-preserved Lower Jurassic section more than 450m thick can be observed (Duarte *et al.*, 2004). This section includes the Toarcian Global Boundary Stratotype Section and Point (GSSP) of the International Commission on Stratigraphy (Rocha *et al.*, 2016) (Fig. 2A). The Triassic–Jurassic boundary is not recognised in Peniche, but marls with gypsum and dolomitic limestones of the Rhaetian–Hettangian Dagorda and Pereiros formations are found at about 10 km to the east in the Óbidos typhonic valley (Alves *et al.*, 2003; Camarate França *et al.*, 1960; Zbyszewski, 1959) (Fig. 1). The first evidence of the Lower Jurassic carbonate platform is found in the Sinemurian Coimbra and Água de Madeiros formations, composed of bioclastic limestones and dolomitic limestones interbedded with marls (Duarte and Soares, 2002; Duarte, 2007). The carbonate sequence includes from bottom to top: bioclastic limestones with brachiopods and bivalves interbedded with centimetre-thick layers of marls (Sinemurian–Pliensbachian Água de Medeiros Formation), marls and limestones with crinoids (Pliensbachian Vale das Fontes Formation), centimetre-thick layers of limestones and marls containing belemnites and ammonites (Pliensbachian Lemedede Formation), and marls and detrital limestones with crinoids (Toarcian Carvoeiro Formation) (Duarte and Soares, 2002; Duarte *et al.*, 2004).

Magmatic activity in the Lusitanian Basin occurred in the Lower Jurassic (c. 200–180Ma) and Cretaceous (c. 147–141 and 94–72Ma) (Fig. 1B; Grange *et al.*, 2008; Kullberg *et al.*, 2013; Miranda *et al.*, 2009). Given the absence of absolute ages, field relations provide the only basis for arguing that the Papôa volcanic breccia is younger than the Lower Jurassic strata. Some authors have pointed to the Cretaceous as the most probable age for this volcanic episode (Andrade, 1979; Romariz, 1963–1964).

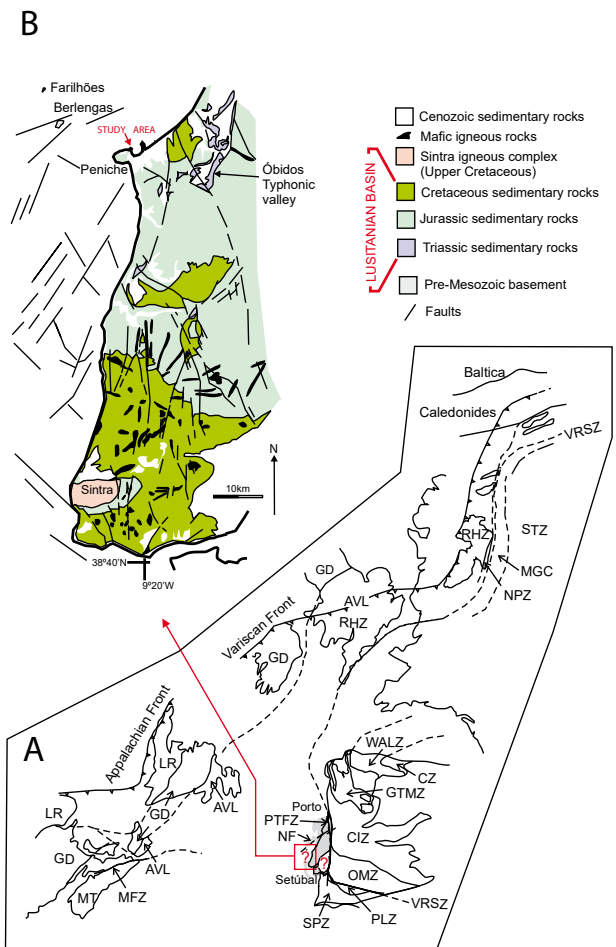


**FIGURE 1.** A) Location of the South-Portuguese (SPZ), Pulo do Lobo (PLZ), Ossa-Morena (SPZ), Galicia-Trás-os-Montes (GTMZ), Central Iberian (CIZ), Cantabrian (CZ) and West Asturian-Leonese (WALZ) zones (Iberian Massif) in the Appalachian-Variscan belt, and adjoining terranes: Saxo-Thuringian (STZ), Northern Phyllite (NPZ) and Rheohercynian (RHZ) zones, Mid-German Crystalline High (MGC), Ganderia (GD), Meguma Terrane (MT), Avalonia (AVL), Laurentia (LR). Modified from Pereira *et al.*, 2017b and references therein. Porto-Tomar Fault Zone (PTFZ), Minas Fault Zone (MFZ), Nazaré Fault (NF). B) Simplified geological map of the Lusitanian Basin and the Berlengas and Farilhões islands (Modified from Camarate França *et al.*, 1960; Oliveira *et al.*, 1992).

### Pre-Mesozoic basement

The structural complexity of the pre-Mesozoic basement of the Iberian Massif, that is unconformably overlain by the Mesozoic Lusitanian Basin, resulted from the progressive amalgamation of different tectonic units during the course of the Gondwana and Laurussia collision, forming the Appalachian-Variscan orogeny (Matte, 2001). In the Iberian Massif, an allochthonous nappe pile formed at c. 390–365Ma as a result of the continental subduction (Galicia-Trás-os-Montes Zone, GTMZ; Martínez Catalán *et al.*, 2019). The following evolutionary stages of this collisional belt (c. 365–315Ma) led to the spatial reorganisation of

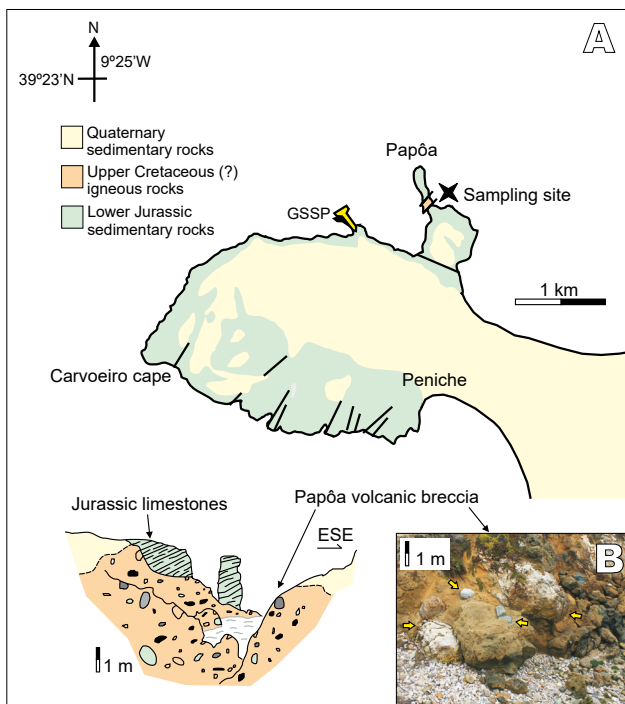


**FIGURE 2.** A) Simplified Geological Map of the Peniche region with location of the sampling site and the Toarcian Global Boundary Stratotype Section and Point (GSSP, Rocha *et al.*, 2016). Modified from Camarate França *et al.*, 1960; Oliveira *et al.*, 1992. B) Sketch of the sampling site of the Papôa volcanic breccia; photograph showing xenoliths (yellow arrows) of different size of carbonate rocks, mafic igneous rocks (basaltic composition?) and granitic rocks.

the different tectonic units derived from the margins of Gondwanan (Central Iberian Zone, CIZ, and Ossa Morena Zone, OMZ) and Laurussian (South Portuguese Zone, SPZ) involved in the Carboniferous collision (Azor *et al.*, 2019).

The latest adjustments to this orogenic system configuration were caused by c. 315–300Ma strike-slip shearing and upright folding related to the waning stages of the continental collision (Díez Fernández and Pereira, 2017; Gutiérrez-Alonso *et al.*, 2015; Martínez Catalán *et al.*, 2007). Regarding the above-mentioned, we might expect that the basement of the Lusitanian Basin would present distinctive characteristics in accordance with the underlying Paleozoic tectonic zone (Pereira *et al.*, 2016), but there is still debate on what this is. The pre-Mesozoic basement flanking the Lusitanian Basin is represented by four tectonic zones showing differences in terms of stratigraphy, deformation, metamorphism, and magmatism: the CIZ, GTMZ, OMZ and SPZ (Martínez-Catalán *et al.*, 2007; Fig. 1A). Stratigraphy of the CIZ and OMZ includes Neoproterozoic to Permian rocks with some significant stratigraphic gaps (Fig. 3). These rocks include Ediacaran successions of greywackes and pelites interbedded with volcanic rocks formed in a magmatic arc (Cadomian orogeny; Pereira *et al.*, 2012; Talavera *et al.*, 2015). In the

OMZ, Cambrian sedimentation is continuous and mostly siliciclastic, including two minor periods of carbonate production (Sánchez García *et al.*, 2019) (Fig. 3). Cambrian siliciclastic rocks and minor carbonate rocks are only represented in the northern and central domains of the CIZ, reaching up to Cambrian Series 2, Stage 4 (Dias da Silva *et al.*, 2014; Gutiérrez-Marco *et al.*, 2019). In both tectonic zones, Ordovician to Lower Devonian marine siliciclastic sedimentation is relevant and include a few unconformities (Gutiérrez-Marco *et al.*, 2019; Robardet and Gutiérrez-Marco, 2004), but Middle Devonian sedimentary rocks are almost absent (Robardet, 2003) (Fig. 3). In the interval c. 530–470Ma magmatism was significant in the OMZ (Díez Fernández *et al.*, 2015; Sánchez-García *et al.*, 2019), while in the CIZ, igneous rocks have yielded Upper Cambrian to Upper Ordovician ages (c. 498–450Ma; Colmenar *et al.*, 2017; Dias da Silva *et al.*, 2015; Montero *et al.*, 2007; Rubio-Ordóñez *et al.*, 2012) (Fig. 3). Furthermore, c. 460–455Ma volcanic rocks are found in the structurally higher GTMZ parautochthonous unit, which presents a stratigraphic record comparable with that of the CIZ (*i.e.* Autochthon) (Dias da Silva *et al.*, 2016). Upper Devonian magmatic rocks and high-grade metamorphism are unknown in the CIZ and OMZ (Fig. 3). The only exception is a few gabbro-dioritic plutons in the OMZ that have yielded questionable ages of  $362 \pm 13$ Ma and  $376 \pm 22$ Ma (Rb-Sr, K-Ar and Sm-Nd ages; Ribeiro *et al.*, 2019). Upper Devonian to Lower Carboniferous marine siliciclastic rocks are overlain by Upper Carboniferous terrestrial strata in the CIZ and OMZ (Martínez-Catalán *et al.*, 2007; Quesada *et al.*, 1990) and by Upper Carboniferous marine strata in the SPZ (Oliveira, 1990; Pereira *et al.*, 2020). Carboniferous and Lower Permian magmatism (c. 350–290Ma) is widespread in the Iberian Massif (Castro *et al.*, 2002; Dias da Silva *et al.*, 2018; Fernández-Suarez *et al.*, 2011; Pereira *et al.*, 2015, 2017a) (Fig. 3). In the western Iberian Massif, the dextral movement of the Porto-Tomar fault zone at c. 310–308Ma (Gutiérrez-Alonso *et al.*, 2015; Pereira *et al.*, 2010) caused the lateral displacement of the adjacent CIZ, OMZ, and SPZ, resulting in a much greater tectonic complexity in the pre-Mesozoic basement of the Lusitanian Basin.

The discussion on the nature of the Paleozoic tectonic unit that constitutes the pre-Mesozoic basement of the Lusitanian Basin is still ongoing, with a number of authors pointing to a range of possibilities: i) the CIZ (Terrinha *et al.*, 2019); ii) the OMZ and CIZ (Oliveira *et al.*, 1992; Pereira *et al.*, 2016); iii) the OMZ and SPZ (Alves, 2011; Capdevila and Mougénou, 1988; Kullberg *et al.*, 2013); iv) the SPZ (Ribeiro *et al.*, 2007); and v) the CIZ, OMZ and SPZ (Pimentel and Pena dos Reis, 2016). However, there is a clue that may help to solve the puzzle. Pre-Mesozoic basement rocks are described in the Berlengas and Farilhões isles as being exposed along a horst on the continental shelf northwest of Peniche (Camarate França *et*

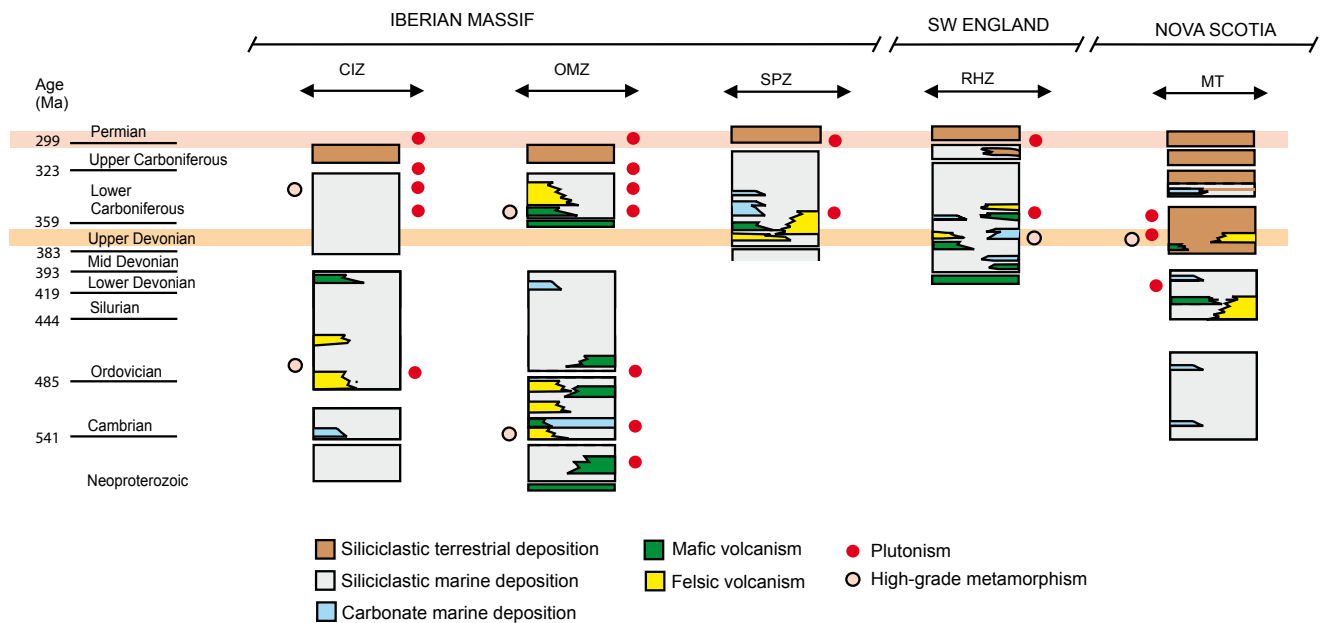


**FIGURE 3.** Summary of the stratigraphy of the Central-Iberian (CIZ), Ossa-Morena (OMZ) and South Portuguese (SPZ) zones (Iberian Massif), and the Renohercynian Zone (RHZ, SW of England) and the Meguma Terrane (MT, Nova Scotia) (modified from Gutiérrez-Marco *et al.*, 2019; Leveridge and Shail, 2011; Murphy *et al.*, 2018; Oliveira and Quesada, 1986; Oliveira, 1990; Pereira *et al.*, 2020; Sánchez García *et al.*, 2019; Shail and Leveridge, 2009; White *et al.*, 2018).

*al.*, 1960; Freire de Andrade, 1937) (Figs. 1B; 2A). Granite from the Berlengas isles was first dated at  $280 \pm 15$  Ma (Rb-Sr whole-rock; Priem *et al.*, 1965) and recently at  $305 \pm 1$  Ma (U-Pb on zircon and monazite fractions; Ribeiro *et al.*, 2019; Valverde-Vaquero *et al.*, 2011). A sample of anatectic granite/diatexite associated with paragneiss migmatites of the Farilhões isles (Bento dos Santos *et al.*, 2010) yielded  $376 \pm 3$  Ma (U-Pb on monazite fractions; Valverde-Vaquero *et al.*, 2011), interpreted as representing the best estimate for the age of high-grade metamorphism. Unfortunately, contact relationships between Berlengas granite and Farilhões high-grade metamorphic rocks have not yet been determined.

## RATIONALE AND SAMPLING

In this study, two fresh xenoliths of granitic rocks were sampled from the Papôa volcanic breccia (Figs. 2B-C; 4A) for the characterization of the pre-Mesozoic basement of the Lusitanian Basin. The aim was to date granitic rocks derived from the underlying basement. Using the new U-Pb data, we aim to discuss: i) the source of the granitic xenoliths, and ii) the relation between the xenoliths of granitic and quartz-feldspathic metamorphic rocks and the Paleozoic basement of the Berlengas and Farilhões isles. If a link between them can be established, as previously suggested by Andrade (1979) and Romariz (1963-1964), a comparative analysis with the pre-Mesozoic basements of

the Appalachian-Variscan belt located both in the Iberian Massif and outside it (Meguma terrane in Nova Scotia and Renohercynian Zone in SW England) could be attempted.

In the study area of Papôa, the NE-SW-trending 30 metres-wide dyke of a matrix-supported mafic breccia cross-cutting the Lower Jurassic strata seems like a sub-vertical volcanic pipe (Fig. 2B). The matrix resembles coarse to fine-grained mafic tuff (Fig. 3A, B) with abundant rock fragments and great variation in size (Figs. 2C; 4A-D). In the dark tuffitic matrix which is commonly intensely altered and replaced by soft yellowish clay, rounded to subangular xenoliths ranging from millimetres to metres in size stand out, (Fig. 4A, B, D). Xenoliths occur in four main groups, each reflecting a different source: i) granitic rocks; ii) quartz-feldspathic foliated rocks (high-grade metamorphic rocks and/or deformed granitic rocks); iii) mafic (basaltic?), pumice, and fine-grained tuffitic rocks; and iv) quartzitic and carbonate hornfels derived from the host sedimentary rocks. Groups i) and ii) represent the deeper crustal sources and often are not easy to distinguish due to the intense weathering. Groups i) and ii) represent the deeper crustal sources and often are not easy to distinguish due to the intense weathering. Group iii) xenoliths are the most abundant, and are derived from sources formed during the subvolcanic process; The two xenoliths of granitic rocks selected for U-Pb geochronology had elongated shapes and were sub-angular to rounded, with a diameter of more than 20 centimetres. They were remarkably fresh, contrary

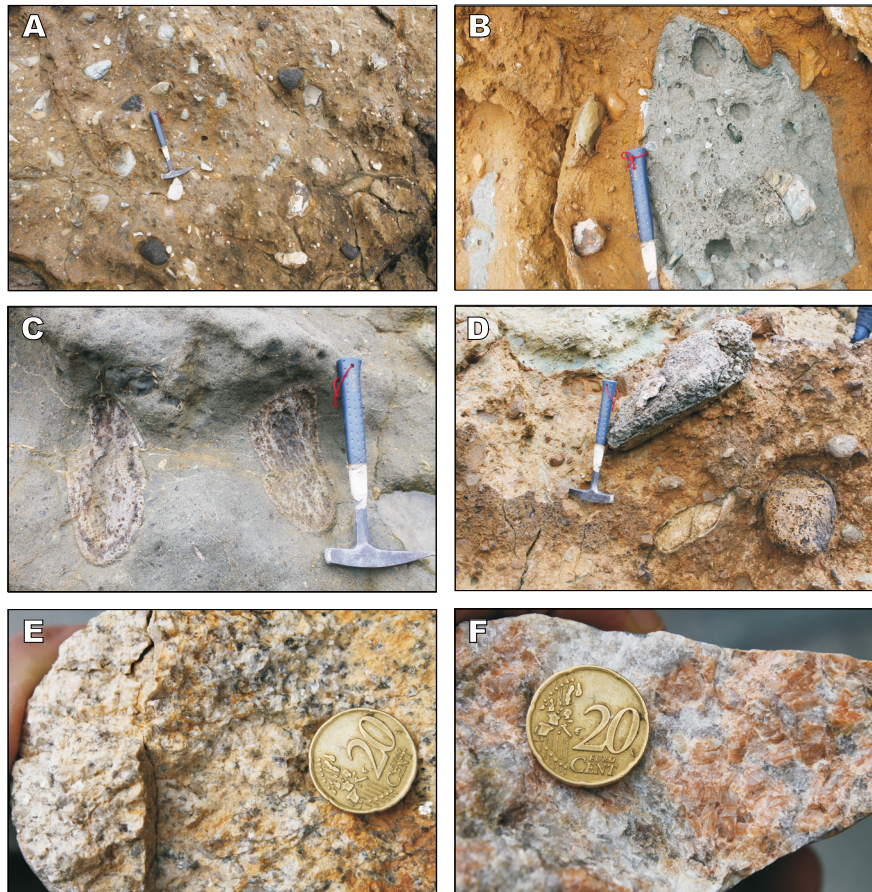


**FIGURE 4.** Photographs of the Papôa volcanic breccia: A-D) distinct types of xenoliths within a tuffitic matrix: A-B) basaltic rocks and quartzitic and carbonate hornfels; C) quartz-feldspathic foliated rocks, carbonate hornfels and basaltic rocks; D) granitic rocks and carbonate hornfels; E) Bt-granite (from sample Xpp-2); F) two-mica granite (from sample Xpp-3); the description of microscopic scale observations of both samples is in the text.

to what is often found due to intense weathering. Sample Xpp-2 coarse-grained biotite granite (Fig. 4E) was mainly composed of quartz, K-feldspar prevailing over plagioclase, and biotite, also including opaque minerals, muscovite, zircon, and apatite. This sample appeared to have been derived from a source with textural and compositional characteristics similar to those of Berlengas granite. Sample Xpp-3 coarse-grained two-mica granite (Fig. 4F), consisted of quartz, K-feldspar, plagioclase, muscovite, and biotite as their main components. It also included monazite, apatite, opaque minerals, and zircon as accessory minerals.

## U-PB GEOCHRONOLOGY

Zircon grains for U-Pb geochronology were selected using traditional techniques: density separation using a sieve with a mesh size of less than 500 microns, density (panning) separation procedures, and mineral identification using a binocular lens and preparation of epoxy resin mounts with zircon grains (Universidade de Évora, Portugal). Cathodoluminescence imaging and U-Pb measurements

using SHRIMP were carried out at IBERSIMS (Universidad de Granada, Spain). Zircon grains were tracked by the primary beam during 120s prior to analysis and then analyzed over 6 scans following the isotope peak sequence  $^{196}\text{Zr}_2\text{O}$ ,  $^{204}\text{Pb}$ , 204.1 backgrounds,  $^{206}\text{Pb}$ ,  $^{207}\text{Pb}$ ,  $^{208}\text{Pb}$ ,  $^{238}\text{U}$ ,  $^{248}\text{ThO}$ ,  $^{254}\text{UO}$ . Every peak of each scan was measured sequentially 10 times: 2s for mass 196; 5s for masses 238, 248, and 254; 15s for masses 204, 206, and 208, and 20s for mass 207. The primary beam, composed of  $^{16}\text{O}^{16}\text{O}^{2+}$ , was set to an intensity of 4-5nA, using a  $120\mu\text{m}$  Kohler aperture, which generates  $17\times 20\mu\text{m}$  elliptical spots on the zircon surface. The secondary beam exit slit was set at  $80\mu\text{m}$ , reaching a resolution of about 5000 at 1% peak height. All calibration procedures were performed on the TEMORA zircon, SL13 zircon, and GAL zircon standards, and mass calibration was done using GAL zircon (ca. 480Ma; Montero *et al.*, 2008). Analytical sessions used SL13 zircon (Claoué-Long *et al.*, 1995) as a concentration standard of U= 238ppm. TEMORA zircon (ca. 417Ma, Black *et al.*, 2003) was used as isotope ratio standard having been subject to measurement every 4 unknowns. Data reduction was accomplished using SHRIMPTOOLS software (www.

ugr.es/fbea). The measured  $^{206}\text{Pb}+^{238}\text{U}+$  and  $\text{UO}^+/\text{U}^+$  ratios were used to calculate  $^{206}\text{Pb}/^{238}\text{U}$  as described by Williams (1998). For high-U zircon grains ( $\text{U}>2500\text{ppm}$ )  $^{206}\text{Pb}/^{238}\text{U}$  was corrected using the algorithm developed by Williams and Hergt (2000). The obtained analytical uncertainties are  $1\sigma$  precision estimates. Ages were estimated using constants suggested by the IUGS Subcommittee on Geochronology (Steiger and Jager, 1977) and the common Pb corrections presumed a model common Pb composition for the age of each spot (Cumming and Richards, 1975). U-Pb results are listed in Table I, see the appendix. Concordia curves and weighted-average means were obtained using Isoplot (Ludwig, 2008), and verified using the TuffZirc algorithm (Ludwig and Mundil, 2002), which is largely insensitive to both Pb loss and inheritance (Figs. 5; 6).

### Xenolith of biotite granite (sample Xpp-2)

Coarse-grained biotite granite (sample Xpp-2) contained stubby-to-elongated euhedral zircon grains (80-350 $\mu\text{m}$  in diameter). Zircon grains mostly showed

well-developed crystal faces. Long prisms had a length-to-width ratio of up to 4:1. CL-imaging showed simple grains with growth zoning typical of magmatic zircon (Corfu *et al.*, 2003) varying from narrow to faint and showing broad zoning. Composite grains included unzoned cores or showed oscillatory growth zoning, banded zoning and sector zoning. The cores were mantled by narrow low-luminescence-to-broad rims with oscillatory zoning (Fig. 5). U and Th ranged from 202 to 3996ppm and from 42 to 1488ppm respectively, and Th/U ranged from 0.02 to 1.4. The average Th/U ratio of 0.4 is typical of igneous origin (Hoskin and Schaltegger, 2003). Of a total of 22 U-Th-Pb isotopic analyses, 15 with a discordance of  $<5\%$  yielded a weighted mean of  $295\pm 5\text{Ma}$  (MSWD=4.2), indicating overdispersion or overestimated uncertainties (Fig. 5). By excluding six analyses (4.1, 9.1, 11.1, 16.1, 18.1 and 21.1), a weighted mean  $^{206}\text{Pb}/^{238}\text{U}$  age of  $298\pm 4\text{Ma}$  (MSWD=1.7) was obtained. This age is interpreted as the best estimate for the crystallisation age of plutonic rock, which coincided within the error with the TuffZirc age of  $299\pm 3\text{Ma}$  (Fig. 5).

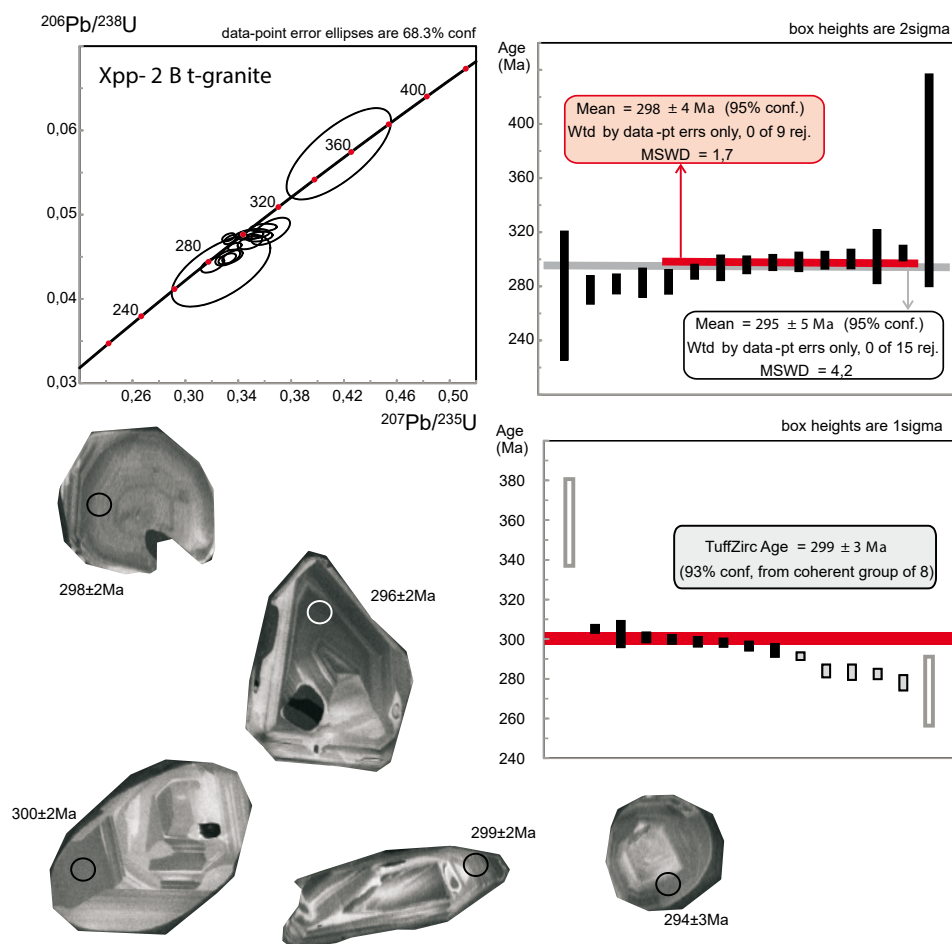


**FIGURE 5.** Concordia diagram, weighted mean of  $^{206}\text{Pb}/^{238}\text{U}$ , and TuffZirc ages of analysed zircon grains of sample Xpp-2 Bt-granite. CL images of representative zircon grains.

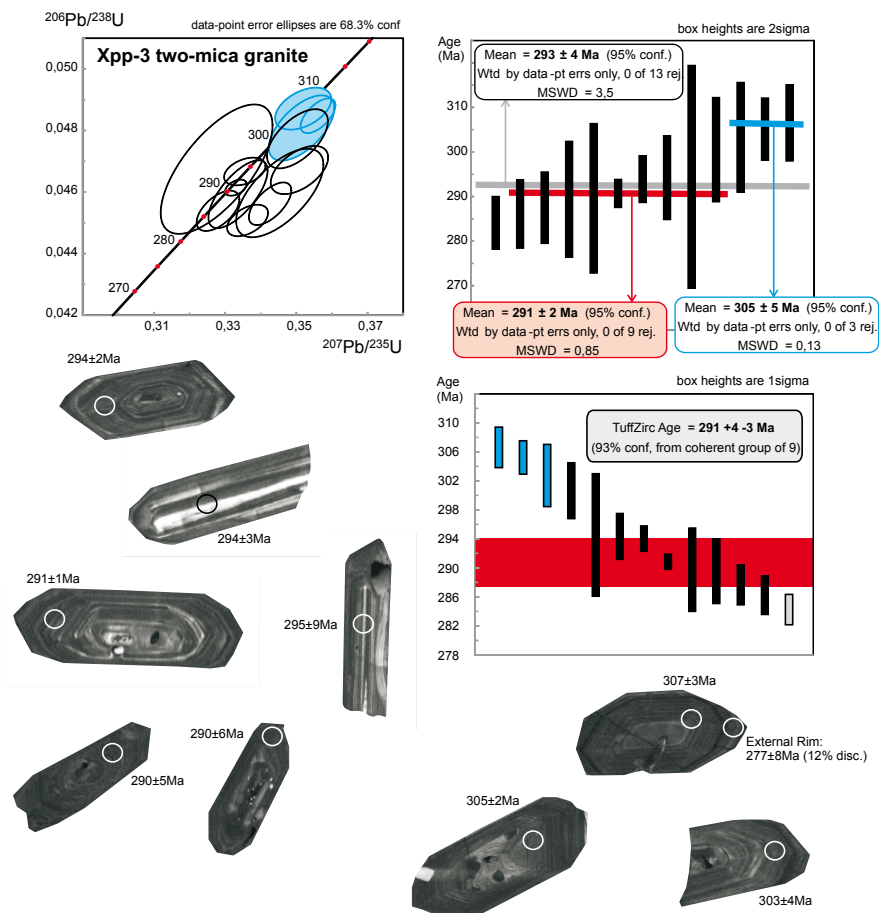


**FIGURE 6.** Concordia diagram (blue ellipses- older ages), weighted mean of  $^{206}\text{Pb}/^{238}\text{U}$ , and TuffZirc ages of analysed zircon grains of sample Xpp-3 two-mica granite. CL images of representative zircon grains.

### Xenolith of two-mica granite (sample Xpp-3)

Coarse-grained two-mica granite (sample Xpp-3) mostly included elongated zircon grains (70–420  $\mu\text{m}$  in diameter) with a few very long prisms and a 6:1 length-to-width ratio. Simple grains showed concentric oscillatory zoning with variable width or banded zoning. CL-imaging demonstrated the complex nature of composite grains, including cores of variable appearance with concentric zoning, banded zoning, and unzoned cores, which were surrounded by rims with concentric oscillatory zoning or were homogeneous and presented low level of luminescence (Fig. 6). A few cores showed the development of irregular domains of homogeneity, cutting discordantly across growth zoned domains, suggesting modifications during late and post-magmatic cooling (Corfu *et al.*, 2003). U content, although variable, was quite high, ranging from 730 to 7847 ppm, while Th values ranged from 99 to 1938 ppm, resulting in Th/U ratios ranging from 0.04 to 1.24 (Table 1), and an average Th/U ratio of 0.26. A total of 18 U-Th-U isotopic analyses, with a discordance of <5%, yielded a weighted mean of  $293 \pm 4 \text{ Ma}$  (MSWD= 3.5) (Fig. 6).

The high MSWD value is associated with the scattering of data points.  $^{207}\text{Pb}/^{206}\text{Pb}$  and  $^{206}\text{Pb}/^{238}\text{U}$  ratios are well defined for a cluster of 10 analyses, yielding a weighted mean age of  $292 \pm 2 \text{ Ma}$  (MSWD= 1.09) and a TuffZirc age of  $291 \pm 4 -3 \text{ Ma}$ , regarded as the crystallisation age of two-mica granite (Fig. 6). In this interpretation, the three older ages that provide a weighted mean of  $305 \pm 5 \text{ Ma}$  (MSWD= 0.13; Fig. 6), probably represent inherited grains from a former zircon forming event. Alternatively, the scattering of data could be explained by the combination of Pb-loss, common Pb correction, and/or recrystallization (*e.g.* Kroner *et al.*, 2014), and thus, the best estimation of the crystallization age of two-mica granite could be c. 305 Ma (*i.e.* similar to the Berlengas granite). A zircon grain showing two oscillatory zoning domains separated by a thin dark unzoned domain was analysed. The most internal oscillatory zoning domain yielded a concordant age of  $307 \pm 3 \text{ Ma}$ , whereas a discordant age of c.  $277 \pm 8 \text{ Ma}$  was obtained for the most external one (Fig. 6), suggesting isotopic disturbance of grain structure. Thus, given the uncertainties of the data set is desirable to quote a maximum (c. 305 Ma) and a minimum (c. 291 Ma) crystallization age for this granitic rock.

## DISCUSSION

The Papôa volcanic breccia, first described by Choffat (1880), has been traditionally interpreted as a fragment of a volcanic cone that was preserved from erosion due to the collapse of a crustal block between two subvertical normal faults (Andrade, 1979). However, our understanding is not the same, admitting that it is a subvertical dike cross-cutting the Lower Jurassic sedimentary host. The most abundant xenoliths in the Papôa volcanic breccia are of mafic tuff and of fine-grained material probably derived from previous crystallization in the dyke walls or representing lava fragments. Mafic xenoliths probably derived from the fragmentation of material from the walls of the subvolcanic pyroclastic dike, and/or from the falling back of pyroclastic material, pumice, welded-tuff, and lava fragments (Kano *et al.*, 1997; Motoki *et al.*, 2012; Winter *et al.*, 2008). Xenoliths of metamorphic rocks mostly comprise carbonate rocks and also siliciclastic rocks derived from the host Mesozoic sedimentary sequence of the Lusitanian Basin. Granitic and quartz-feldspathic foliated rocks also occur as xenoliths, representing the pre-Mesozoic basement of the Peniche region (Fig. 7A). Xenoliths of granitic rocks present little compositional variation but show significant textural differences, including aplitic and pegmatitic textures. In some cases, they are altered and difficult to distinguish from quartz-feldspathic metamorphic rocks. These xenoliths of granitic rocks and quartz-feldspathic foliated metamorphic rocks, of probable upper and middle crust provenance, are comparable lithologically and geochemically to the pre-Mesozoic basement rocks forming the Berlengas and Farilhões isles (Camarate França *et al.*, 1960; Freire de Andrade, 1937; Rosa *et al.*, 2019) (Fig. 7B).

The new geochronology data obtained from the granitic xenoliths of the Papôa volcanic breccia show that the pre-Mesozoic basement of the Lusitanian Basin includes Permo-Carboniferous granites (c. 298 and 305-291Ma; this study). A number of provenance hypotheses may be advanced to explain the presence of xenoliths of Permian granitic rocks in the Papôa volcanic breccia. In the Iberian Massif, Permian magmatism is present throughout the CIZ (Fernández Suarez *et al.*, 2011), OMZ (Pereira *et al.*, 2017a), and SPZ (Braid *et al.*, 2012; Díez Montes *et al.*, 2017), therefore they may all be regarded constituting the Lusitanian Basin pre-Mesozoic basement.

In a Late Carboniferous paleogeographic reconstruction (Stampfli *et al.*, 2013) the SPZ is probably the continuation of the Meguma Terrane (Nova Scotia) before the opening of the Atlantic Ocean. The SPZ has usually been associated with the Meguma terrane (Braid *et al.*, 2012; Domeier and Torsvik, 2014; Nance *et al.*, 2015; Pereira *et al.*, 2017b) and the Rhenohercynian Zone of southwest England (Matte, 2001; Oliveira and Quesada, 1988; Shail and Leveridge,

2009), which suggests that it was part of the Laurussian margin before the collision with the Gondwanan margin (OMZ and CIZ). In the Rhenohercynian Zone, there is the Permian Cornubian Batholith, 250km long, 20-40km wide and 5-10km thick, hosted by Early Devonian to Late Carboniferous marine sedimentary rocks with subordinate volcanic rocks (Simons *et al.*, 2016). Farther south, these Devonian and Carboniferous rocks (Leveridge and Hartley, 2006), are in contact with the c. 397Ma Lizard ultramafic-mafic Complex, that records a history of magmatism and metamorphism extending at least from c. 397Ma to c. 370Ma (Clarke *et al.*, 2003; Leveridge and Shail, 2011).

The Cornubian Batholith comprises six major plutons and several minor stocks emplaced coevally with lamprophyric dykes and basaltic lava flows, indicating about 20Ma of magmatic activity, from c. 294 to 274Ma (Chesley *et al.*, 1993; Clark *et al.*, 1994; Dupuis *et al.*, 2015). Permo-Carboniferous ages were also recognised in a few plutons (c. 308-301Ma; Braid *et al.*, 2012; Díez Montes *et al.*, 2017) that are associated with the Sierra Norte Batholith of the eastern SPZ. Berlengas granite, dated at 305±0.5Ma (monazite and zircon fractions; Valverde-Vaquero *et al.*, 2011), and the two xenoliths of granite from the Papôa volcanic breccia (c. 298Ma and c. 305-291Ma, this study) coincide within the margin of error with the age of crystallisation of the Permo-Carboniferous plutons of the SPZ and Rhenohercynian Zone. Permian igneous activity is not recognised in the Meguma terrane (Don Hermes and Murray, 1988). Meguma terrane stratigraphy includes Cambrian to Early Ordovician sedimentary rocks unconformably overlain by Silurian-Early Devonian sedimentary and volcanic rocks dated at c. 446-434Ma (Keppie and Krogh 2000; White and Barr, 2012; White *et al.*, 2018).

This Early Paleozoic succession may represent the covered, unknown oldest stratigraphic record of the SPZ in the southwest Iberian Massif. In the Meguma terrane, the Early Paleozoic sequence is intruded by c. 382-357Ma plutons (including the South Mountain and Musquodoboit batholiths, Clarke *et al.*, 1997; Tate and Clarke, 1995). In Nova Scotia, the Late Devonian sequence comprises sedimentary rocks interbedded with volcanic rocks (Doig *et al.*, 1996; Murphy *et al.*, 2018; Pe-Piper *et al.*, 2004). Zircon and monazite U-Pb ages obtained from granulite facies metasedimentary xenoliths from a Late Devonian mafic dyke that intrudes the Meguma terrane, yielded three age groups at c. 399, 377 and 354Ma, interpreted as representing metamorphic events (Greenough *et al.*, 1999; Shellnutt *et al.*, 2018). One of these three age groups recorded in the Meguma terrane was contemporaneous with the widespread plutonism (c. 378-368Ma) that involves the mafic stocks and large granitic plutons of the Musquodoboit and South Mountain

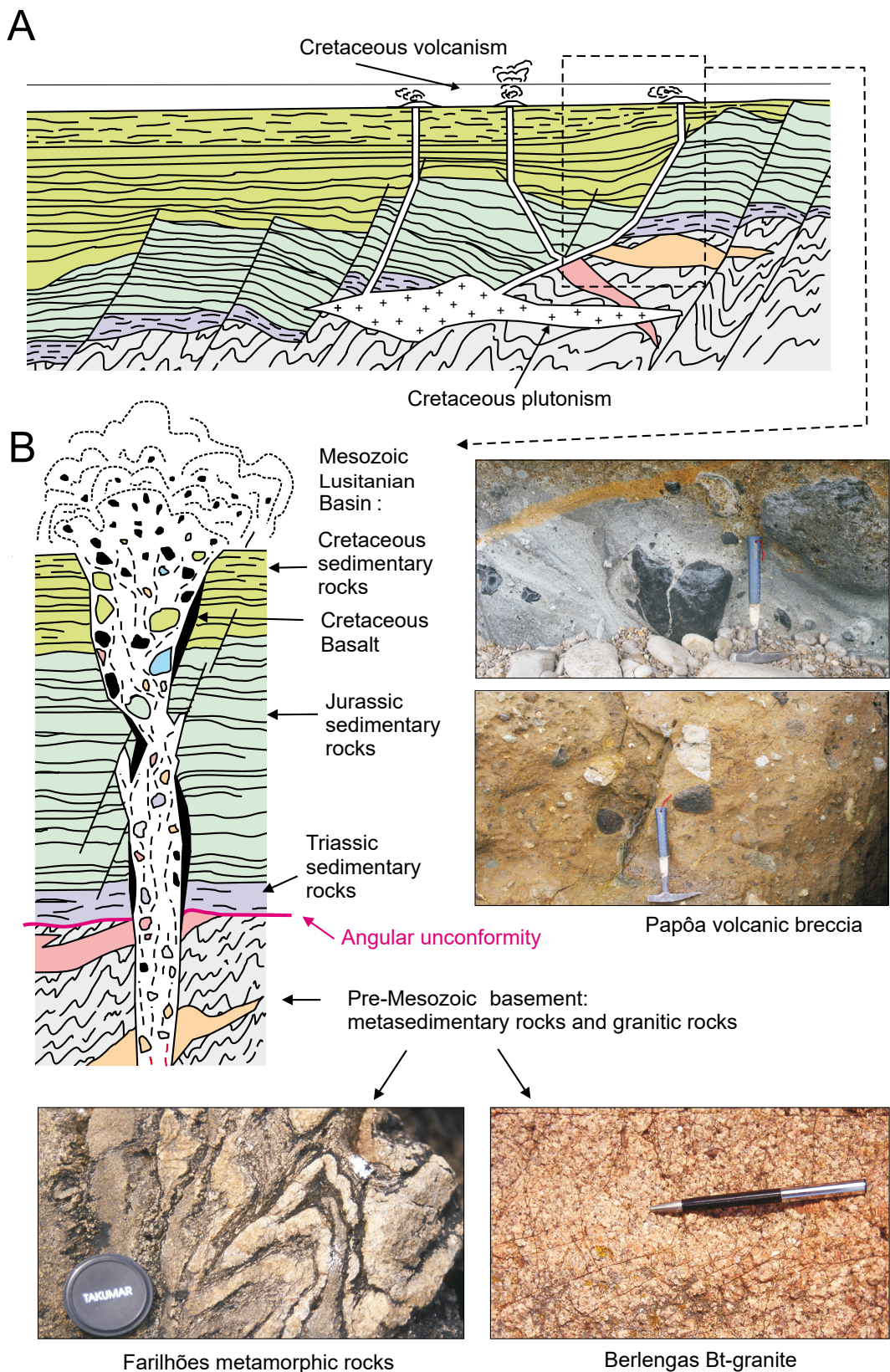


**FIGURE 7.** A) Sketch of the Lusitanian Basin stratigraphy overlying the pre-Mesozoic basement, showing the contact between the active feeder dyke and the host-rock sequences; B) Schematic sketch of the Papôa pyroclastic eruption showing entrapment of xenoliths, derived from distinct sources, in the ascending magmas.

batholiths (Moran *et al.*, 2007). It deserves special mention because the metamorphic rocks of the Farilhões isles also experienced high-grade metamorphic conditions under granulite facies (Ribeiro *et al.*, 2019) dated at  $376 \pm 3$  Ma (Valverde Vaquero *et al.*, 2011). By contrast, Late Devonian high-grade metamorphism has not been reported in the OMZ and CIZ (Fig. 3). Furthermore, U-Pb geochronology of magmatic rocks from the Iberian Pyrite Belt (Oliveira *et al.*, 2013; Paslawski *et al.*, 2020; Rosa *et al.*, 2008) and the Sierra Norte Batholith (Braid *et al.*, 2012; Gladney *et al.*, 2014; De la Rosa *et al.*, 2002) in the SPZ, likewise provided Late Devonian-Early Carboniferous ages of c. 374–335 Ma. Whatever the case, as there are no dating for xenoliths of foliated quartz-feldspathic rocks, we cannot rule out the hypothesis that they may represent high degrees of partial melting of the basement entrapped in ascending magma (Dostal *et al.*, 2005) contemporaneous with the formation of Papôa volcanic breccia. A detailed petrographic and geochronological study of the different sedimentary rocks and quartz-feldspathic xenoliths remains to be carried out.

## CONCLUSIONS

The age of the granitic xenoliths from the Papôa volcanic breccia (c. 298 and c. 305–291 Ma) corroborates the previous hypotheses, based on field, petrography, geochemical, and geochronology data, that the Lusitanian Basin rests on a pre-Mesozoic basement that includes Permo-Carboniferous intrusions like those described in the Berlengas and Farilhões isles. This enable us to posit that: i) Permo-Carboniferous magmatism probably lasted at least 14 Ma, from c. 305 to 291 Ma, in this region, similarly to what happened in others regions of the Appalachian-Variscan belt; and ii) the Lusitanian Basin basement was affected by the Permo-Carboniferous granite intrusion and Upper Devonian high-grade metamorphism and magmatism, as evident in the Paleozoic terrain with Laurussian affinity including the SPZ, the Rhenohercynian Zone and the Meguma terrane. The present study thus confirms that the pre-Mesozoic basement represented by the OMZ and CIZ (Gondwana) was still connected to SPZ-Rhenohercynian Zone-Meguma Terrane (Laurussia) during the Mesozoic evolution of the Lusitanian Basin. Thus, the rifting that led to the opening of the Central Atlantic Ocean left behind large fragments of Paleozoic Laurussian continental material stranded in the western Iberian margin.

## ACKNOWLEDGMENTS

MFP and CG acknowledge the financial support by the Portuguese Foundation for Science and Technology (FCT) project UIDB/04683/2020-ICT (Universidade de Évora). IDS acknowledges the financial support by the “Estímulo

ao Emprego Científico-Norma Transitória” national science contract, Faculdade de Ciências da Universidade de Lisboa. This work is a contribution to the IGCP project 648, IDL’s Research Group 3 (Solid Earth dynamics, hazards and resources), and to IDL’s FCT-projects UID/GEO/50019/2019-IDL and UIDB/50019/2020-IDL. We thank Pablo Valverde-Vaquero for his careful revision that has contributed decisively to improve the content of this manuscript, the interpretation of geochronology data in particular. This is the IBERSIMS publication N° 76.

## REFERENCES

- Alves, T.M., Manuppella, G., Gawthorpe, R.L., Hunt, D.W., Monteiro, J.H., 2003. The depositional evolution of diapir- and fault-bounded rift basins: examples from the Lusitanian Basin of West Iberia. *Sedimentary Geology*, 162, 273–303.
- Alves, S.L., 2011. Contribuição dos métodos potenciais para os estudos tectónicos regionais na Margem Continental Ibérica Ocidental. *Boletim Geociências Petrobras*, 19(1-2), 53–68.
- Andrade, M.M., 1979. O tufo-brecha da Papôa: resto dum cone vulcânico de piroclastitos? *Publicações do Museu e Laboratório Mineralógico e Geológico da Faculdade de Ciências do Porto*, XCI, 4ª série, 214–222.
- Azor, A., Dias da Silva, Í., Gómez Barreiro, J., González-Clavijo, E., Martínez Catalán, J.R., Simancas, J.F., Martínez Poyatos, D., Pérez-Cáceres, I., González Lodeiro, F., Expósito, I., Casas, J.M., Clariana, P., García-Sansegundo, J., Margalef, A., 2019. Deformation and Structure. In: Quesada, C., Oliveira, J.T. (eds.). *The Geology of Iberia: A Geodynamic Approach*. Volume 2: The Variscan Cycle. Springer International Publishing, 307–348.
- Bento dos Santos, T., Ribeiro, M.L., Clavijo, E., Díez Montes, A., Solá, A.R., 2010. Estimativas geotermobarométricas e percursos P-T de migmatitos dos Farilhões, Arquipélago das Berlengas, Oeste de Portugal. e-Terra. *Revista Eletrónica de Ciências da Terra*, 16(11), Extended abstract, 4.
- Black, L.P., Kamo, S.L., Allen, C.M., Aleinikoff, J.A., Davis, D.W., Korsch, J.R., Foudolis, C., 2003. TEMORA 1: a new zircon standard for Phanerozoic U-Pb geochronology. *Chemical Geology*, 200, 155–170.
- Braid, J.A., Murphy, J.B., Quesada, C., Bickerton, L., Mortensen, J.K., 2012. Probing the composition of unexposed basement, South Portuguese Zone, Southern Iberia: implications for the connections between the Appalachian and Variscan orogens. *Canadian Journal of Earth Sciences*, 49, 591–613.
- Camarate França, J., Zbyszewski, G., Almeida, F.M., 1960. Carta Geológica de Portugal na escala 1/50000, folha 26-C (Peniche). *Serviços Geológicos de Portugal*.
- Capdevilla, R., Mougénot, D., 1988. Pre-Mesozoic basement of the Western Iberian continental margin and its place in the Variscan Belt. In: Boillot, G., Winterer, E.L., Meyer, A.W., and Shipboard Scientific party (eds.). *Proceedings of the Ocean Drilling Program*. Scientific results, 103, 3–12.

- Castro, A., Corretgé, L.G., De La Rosa, J., Enrique, P., Martínez, E.J., Pascual, E., Lago, M., Arranz, E., Galé, C., Fernández, C., Donaire, T., López, S., 2002. Paleozoic magmatism. In: Gibbons, W., Moreno, M.T. (eds.). *The Geology of Spain*. London, Geological Society, 117-153.
- Chesley, J.T., Halliday, A.N., Snee, L.W., Mezger, K., Shepherd, T.J., Scrivener, R.C., 1993. Thermochronology of the Cornubian Batholith in southwest England: implications for pluton emplacement and protracted hydrothermal mineralisation. *Geochimica et Cosmochimica Acta*, 57, 1817-1835.
- Choffat, P.L., 1880. Étude stratigraphique et paléontologique des terrains jurassiques du Portugal. Première livraison- Le Lias et le Dogger au Nord du Tage. *Memórias Secções Trabalhos Geológicos de Portugal*, 22, 72pp.
- Claoué-Long, J.C., Compston, W., Roberts, J., Fanning, C.M., 1995. Two Carboniferous ages: a comparison of SHRIMP zircon dating with conventional zircon ages and  $^{40}\text{Ar}/^{39}\text{Ar}$  analyses. In: Berggren, W.A., Kent, D.V., Aubry, M.-P., Hardenbol, J. (eds.). *Geochronology, Time Scales and Global Stratigraphic Correlation*. SEPM (Society of Sedimentary Petrology), 54 (Special Publication), 3-21.
- Clark, A.H., Chen, Y., Farrar, E., Northcote, B., 1994. Refinement of the time-space relationships of intrusion and hydrothermal activity in the Cornubian Batholith. *Proceedings of the Ussher Society*, Abstract, 345.
- Clarke, D.B., MacDonald, M.A., Tate, M.C., 1997. Late Devonian Mafic-felsic Magmatism in the Meguma Zone, Nova Scotia. In: Sinha, A.K., Whalen, J.B., Hogan, J.P. (eds.). *The Nature of Magmatism in the Appalachian Orogen*. Geological Society of America Memoir, 191, 107-127.
- Clarke, D.B., MacDonald, M.A., Reynolds, P.H., Longstaffe, E.I., 2003. Leucogranites from the eastern part of the South Mountain Batholith, Nova Scotia. *Journal of Petrology*, 34, 653-679.
- Colmenar, J., Pereira, S., Sá, A.A., da Silva, C.M., Young, T.P., 2017. The highest-latitude Foliomena Fauna (Upper Ordovician, Portugal) and its palaeogeographical and palaeoecological significance. *Palaeogeography Palaeoclimatology Palaeoecology*, 485, 774-783.
- Corfu, F., Hanchar, J.M., Hoskin, P.W.O., Kinny, P., 2003. Atlas of Zircon Textures. *Reviews in Mineralogy and Geochemistry*, 53, 468-500.
- Cumming, G.L., Richards, J.R., 1975. Ore lead isotope ratios in a continuously changing earth. *Earth Planetary Science Letters*, 28, 155-171.
- De la Rosa, J.D., Jenner, G.A., Castro, A., 2002. A study of inherited zircon in granitoid rocks from the South Portuguese and Ossa-Morena Zones, Iberian Massif: support for the exotic origin of the South Portuguese Zone. *Tectonophysics*, 352, 245-256.
- Dias da Silva, Í., Pereira, M.F., Silva, J.B., Gama, C., 2018. Time-space distribution of silicic plutonism in a gneiss dome of the Iberian Variscan Belt: The Évora Massif (Ossa-Morena Zone, Portugal). *Tectonophysics*, 747-748, 298-317.
- Dias da Silva, Í., Jensen, S., González Clavijo, E., 2014. Trace fossils from the Desejosa Formation (Schist and Greywacke Complex, Douro Group, NE Portugal): new Cambrian age constraints. *Geologica Acta*, 12(2), 109-120.
- Dias da Silva, Í., Díez Fernández, R., Díez-Montes, A., González Clavijo, E., Foster, D.A., 2016. Magmatic evolution in the N-Gondwana margin related to the opening of the Rheic Ocean-evidence from the Upper Parautochthon of the Galicia-Trás-os-Montes zone and from the Central Iberian zone (NW Iberian Massif). *International Journal of Earth Sciences*, 105, 1127-1151.
- Díez Fernández, R., Pereira, M.F., 2017. Strike-slip shear zones of the Iberian Massif: Are they coeval? *Lithosphere* 9(5), 726-744.
- Díez Fernández, R., Pereira, M.F., Foster, D.A., 2015. Peralkaline and alkaline magmatism of the Ossa-Morena zone (SW Iberia): age, source, and implications for the Paleozoic evolution of Gondwanan lithosphere. *Lithosphere*, 7, 73-90.
- Díez Montes, A., Valverde-Vaquero, P., Rey-Moral, C., Sánchez García, T., 2017. Late Variscan, Permo-Carboniferous, Al-K plutonism in the South Portuguese Zone: El Crispinejo cordierite-bearing granite. *Geologica Acta*, 15(4), 429-442.
- Doig, R., Murphy, J.B., Pe-Piper, G., Piper, D.J.W., 1996. U-Pb geochronology of Late Palaeozoic plutons, Cobequid Highlands, Nova Scotia, Canada: evidence for Late Devonian emplacement adjacent to the Meguma-Avalon terrane boundary in the Canadian Appalachians. *Geological Journal*, 31, 179-188.
- Domeier, M., Torsvik, T.H., 2014. Plate tectonics in the late Paleozoic. *Geoscience Frontiers*, 5, 303-350.
- Don Hermes, O., Murray, D.P., 1988. Middle Devonian to Permian plutonism and volcanism in the N American Appalachians. London, Geological Society, 38 (Special Publications), 559-571.
- Dostal, J., Keppie, J.D., Hamilton, M.A., Aarab, E.M., Lefort, J.P., Murphy, J.B., 2005. Crustal xenoliths in Triassic lamprophyre dykes in western Morocco: tectonic implications for the Rheic Ocean suture. *Geological Magazine*, 142(2), 159-172.
- Duarte, L.V., Soares, A.F., 2002. Litostratigrafia das séries margo-calcárias do Jurássico inferior da Bacia Lusitânica (Portugal). *Comunicações Instituto Geológico e Mineiro*, 89, 135-154.
- Duarte, L.V., Wright, V.P., Fernández-López, S., Elmi, S., Krautter, M., Azerêdo, A.C., Henriques, M.H., Rodrigues, R., Perilli, N., 2004. Early Jurassic carbonate evolution in the Lusitanian Basin: facies, sequence stratigraphy and cyclicity. In: Duarte, L.V., Henriques, M.H. (eds.). *Carboniferous and Jurassic Carbonate Platforms of Iberia*. 23rd IAS Meeting of Sedimentology, Coimbra. Field Trip Guide Book, Volume I, 45-71.
- Duarte, L.V., 2007. Lithostratigraphy, sequence stratigraphy and depositional setting of the Pliensbachian and Toarcian series in the Lusitanian Basin (Portugal). In: Rocha, R.B. (ed.). *The Peniche section (Portugal)*. Contributions to the definition of the Toarcian GSSP International Subcommittee on Jurassic Stratigraphy, 17-23.
- Dupuis, N.E., Braid, J.A., Murphy, J.B., Shail, R.K., Archibald, D.A., Nance, R.D., 2015.  $^{40}\text{Ar}/^{39}\text{Ar}$  phlogopite geochronology of lamprophyre dykes in Cornwall, UK: new age constraints on Early Permian post-collisional magmatism

- in the Rheohercynian Zone, SW England. *Journal of the Geological Society*, 172, 566-580.
- Fernández-Suárez, J., Gutiérrez-Alonso, G., Johnston, S.T., Jeffries, T.E., Pastor-Galan, D., Jenner, G.A., Murphy, J.B., 2011. Iberian late-Variscan granitoids: Some considerations on crustal sources and the significance of “mantle extraction ages”. *Lithos*, 123, 121-132.
- Freire de Andrade, C., 1937. Os Vales Submarinos Portugueses e o Diastrofismo das Berlengas e da Estremadura. *Serviços Geológicos de Portugal*, 235pp.
- Gladney, E.R., Braid, J.A., Murphy, J.B., Quesada, C., McFarlane, C.R.M., 2014. U–Pb geochronology and petrology of the Late Paleozoic Gil Márquez pluton: magmatism in the Variscan suture zone, southern Iberia, during continental collision and the amalgamation of Pangea. *International Journal of Earth Sciences*, 103, 1433-1451.
- Grange, M., Scharer, U., Comen, G., Girardeau, J., 2008. First alkaline magmatism during Iberia-Newfoundland rifting. *Terra Nova*, 20, 494-503.
- Greenough, J.D., Krogh, T.E., Kamo, S.L., Owen, J.V., Ruffman, A., 1999. Precise U-Pb dating of Meguma basement xenoliths: new evidence for Avalonian underthrusting. *Canadian Journal of Earth Sciences*, 36, 15-22.
- Gutiérrez-Alonso, G., Collins, A.S., Fernández-Suárez, J., Pastor-Galán, D., González-Clavijo, E., Jourdan, F., Weil, A.B., Johnston, S.T., 2015. Dating of lithospheric buckling: 40Ar/39Ar ages of syn-orocline strike-slip shear zones in northwestern Iberia. *Tectonophysics*, 643, 44-54.
- Gutiérrez-Marco, J.C., Piçarra, J.M., Meireles, C.A., Cózar, P., García-Bellido, D.C., Pereira, Z., Vaz, N., Pereira, S., Lopes, G., Oliveira, J.T., Quesada, C., Zamora, S., Esteve, J., Colmenar, J., Bernárdez, E., Coronado, I., Lorenzo, S., Sá, A.A., Dias da Silva, Í., González-Clavijo, E., Díez-Montes, A., Gómez-Barreiro, J., 2019. Early Ordovician–Devonian Passive Margin Stage in the Gondwanan Units of the Iberian Massif. In: Quesada, C., Oliveira, J.T. (eds.). *The Geology of Iberia: A Geodynamic Approach. Volume 2: The Variscan Cycle*. Springer International Publishing, 75-98.
- Hoskin, P.W.O., Schaltegger, U., 2003. The composition of zircon and igneous and metamorphic petrogenesis. *Reviews in Mineralogy and Geochemistry*, 53, 27-62.
- Kano, K., Matsuura, H., Yamauchi, S., 1997. Miocene rhyolitic welded tuff infilling a funnel-shaped eruption conduit Shiotani, southeast of Matsue, SW Japan. *Bulletin of Volcanology*, 59, 125-135.
- Keppie, J.D., Krogh, T.E., 2000. 440 Ma igneous activity in the Meguma terrane, Nova Scotia, Canada: part of the Appalachian overstep sequence? *American Journal of Science*, 300, 528-538.
- Kullberg, J.C., Rocha, R.B., Soares, A.F., Rey, J., Terrinha, P., Azerêdo A.C., Callapez, P., Duarte, L.V., Kullberg, M.C., Martins, L., Miranda, J.R., Alves, C., Mata, J., Madeira, J., Mateus, O., Moreira, M., Nogueira, C.R., 2013. A Bacia Lusitaniana: Estratigrafia, Paleogeografia e Tectónica. In: Dias, R., Araújo, A., Terrinha, P., Kullberg, J.C. (eds.). *Geologia de Portugal no contexto da Ibéria*. Escolar Editora, 195-347.
- Leveridge, B.E., Shail, R.K., 2011. The Gramscatho Basin, south Cornwall, UK: Devonian active margin successions. *Proceedings of the Geologists' Association*, 122, 568-615.
- Leveridge, B.E., Hartley, A.J., 2006. The Variscan Orogeny: the development of Devonian/Carboniferous basins in SW England and South Wales. In: Brenchley, P.J., Rawson, P.F. (eds.). *The Geology of England and Wales*. Geological Society of London, 2nd ed., 225-255.
- Ludwig, K.R., 2008. *Isoplot/Ex Version 3.70: a Geochronological Toolkit for Microsoft Excel*, Berkeley Geochronology Center Special Publication No. 4.
- Ludwig, K.R., Mundil, R., 2002. Extracting reliable U-Pb ages and errors from complex populations of zircons from Phanerozoic tuffs. *Geochimica et Cosmochimica Acta*, v. 66, 463.
- Martínez Catalán, J.R., Gómez Barreiro, J., Dias da Silva, Í., Chichorro, M., López-Carmona, A., Castiñeras, P., Abati, J., Andonaegui, P., Fernández-Suárez, J., González Cuadra, P., Benítez-Pérez, J.M., 2019. Variscan Suture Zone and Suspect Terranes in the NW Iberian Massif: Allochthonous Complexes of the Galicia-Trás os Montes Zone (NW Iberia). In: Quesada, C., Oliveira, J.T. (eds.). *The Geology of Iberia: A Geodynamic Approach. Volume 2: The Variscan Cycle*. Springer International Publishing, 99-130.
- Martínez-Catalán, J.R., Arenas, R., Diaz Garcia, F., Gomez-Barreiro, J., Abati, J., Castiñeras, P., Fernández-Suárez, J., Sánchez Martínez, S., Adanaegui, P., 2007. Space and Time in the Tectonic Evolution of the Northwestern Iberian Massif. Implications for the Comprehension of the Variscan Belt. In: Hatcher Jr., R.D., Carlson, M.P., McBride, J.H., Martinez-Catalan, J.R. (eds.). *4-D Framework of Continental Crust*. Boulder (Colorado), Geological Society of America Memoir 200, 403-423.
- Matte, P., 2001. The Variscan collage and orogeny (480-290 Ma) and the tectonic definition of the Armorica microplate: a review. *Terra Nova*, 13, 122-128.
- Miranda, R., Valadares, V., Terrinha, P., Mata, J., Azevêdo, M.R., Gaspar, M., Kullberg, J.C., Ribeiro, C., 2009. Age constrains on the Late Cretaceous alkaline magmatism on the West Iberian Margin. *Cretaceous Research*, 30, 575-586.
- Montero, M.P., Bea, E., Corretge, L.G., Floor, P., Whitehouse, M.J., 2008. U-Pb ion microprobedating and Sr-Nd isotope geology of the Galiñeiro Igneous Complex. A model for the peraluminous/peralkaline duality of the Cambro-Ordovician magmatism of Iberia. *Lithos*, 107, 227-238.
- Montero, P., Bea, E., González-Lodeiro, F., Talavera, C., Whitehouse, M.J., 2007. Zircon ages of the metavolcanic rocks and metagranites of the Ollo de Sapo Domain in central Spain: Implications for the Neoproterozoic to Early Palaeozoic evolution of Iberia. *Geological Magazine*, 144, 963-976.
- Moran, P.C., Barr, S.M., White, C.E., Hamilton, M.A., 2007. Petrology, age, and tectonic setting of the Seal Island Pluton, offshore southwestern Nova Scotia. *Canadian Journal of Earth Sciences*, 44, 1467-1478.
- Motoki, A., Geraldes, M.C., Iwanuch, W., Vargas, T., Motoki, K.E., Balmant, A., Ramos, M.N., 2012. The pyroclastic dyke and

- welded crystal tuff of the Morro dos Gatos alkaline intrusive complex, State of Rio de Janeiro, Brazil. *Revista da Escola de Minas, Ouro Preto, Geociências*, 65(1), 35-45.
- Murphy, J.B., Shellnutt, J.G., Collins, W.J., 2018. Late Neoproterozoic to Carboniferous genesis of A-type magmas in Avalonia of northern Nova Scotia: repeated partial melting of anhydrous lower crust in contrasting tectonic environments. *International Journal of Earth Sciences*, 107, 587-599.
- Nance, R.D., Neace, E.R., Braid, J.A., Murphy, B., Dupuis, N., Shail, R.K., 2015. Does the Meguma Terrane extend into SW England? *Journal of the Geological Association of Canada*, 42, 61-76.
- Oliveira, J.T., 1990. Stratigraphy and Synsedimentary Tectonism in the South Portuguese Zone. In: Dallmeyer, R.D., Martínez, E. (eds.). *Pre-Mesozoic Geology of Iberia*. Berlin (Heidelberg), Springer Verlag, 334-347.
- Oliveira, J.T., Quesada, C., 1986. A comparison of stratigraphy, structure and palaeogeography of the South Portuguese Zone and south-west England, European Variscides. *Geoscience in south-west England*, 9, 141-150.
- Oliveira, J.T., Pereira, E., Ramalho, M., Antunes, M.T., Monteiro, J.H., 1992. Carta Geológica de Portugal, escala 1/500 000. Lisboa, Serviços Geológicos de Portugal.
- Oliveira, J.T., Rosa, C.J.P., Pereira, Z., Rosa, D.R.N., Matos, J.X., Inverno, C.M.C., Andersen, T., 2013. Geology of the Rosário-Neves Corvo antiform, Iberian Pyrite Belt, Portugal: new insights from physical volcanology, palynostratigraphy and isotope geochronology studies. *Mineralium Deposita*, 48, 749-766.
- Palain, C., 1976. Une série détritique terrigène, les "Grés de Silves": Trias et Lias inférieur du Portugal. *Memórias dos Serviços Geológicos de Portugal, Lisboa, Nova Serie*, 25, 377pp.
- Paslawski, L.E., Braid, J.A., Quesada, C., McFarlane, C.M., 2020. Geochronology of the Iberian Pyrite Belt and the Sierra Norte Batholith: Lower Plate Magmatism during Supercontinent Amalgamation? In: Murphy, J.B., Strachan, R.A., Quesada, C. (eds.). *Pannotia to Pangaea: Neoproterozoic and Paleozoic Orogenic Cycles in the Circum-Atlantic Region*. London, Geological Society, 503 (Special Publications). DOI: <https://doi.org/10.1144/SP503-2020-5>
- Pe-Piper, G., Reynolds, P.H., Nearing, J., Piper, D.J.W., 2004. Evolution of a Late Paleozoic shear zone in the Cobequid Highlands, Nova Scotia: an  $^{40}\text{Ar}/^{39}\text{Ar}$  geochronology study. *Canadian Journal of Earth Sciences*, 41, 1425-1436.
- Pereira, M.F., Silva, J.B., Drost, K., Chichorro, M., Apraiz, A., 2010. Relative timing of transcurrent displacements in northern Gondwana: New U-Pb laser ablation MS-ICP-MS zircon and monazite geochronology of gneisses and sheared granites from the Western Iberian Massif (Portugal). *Gondwana Research*, 17(2-4), 461-481.
- Pereira, M.F., Linnemann, U., Hofmann, M., Chichorro, M., Solá, A.R., Medina, J., Silva, J.B., 2012. The provenance of Late Ediacaran and Early Ordovician siliciclastic rocks in the Southwest Central Iberian zone: Constraints from detrital zircon data on northern Gondwana margin evolution during the late Neoproterozoic. *Precambrian Research*, 192-195, 166-189.
- Pereira, M.F., Chichorro, M., Moita, P., Santos, J.F., Solá, A.M.R., Williams, I.S., Silva, J.B., Armstrong, R.A., 2015. The multistage crystallization of zircon in calc-alkaline granitoids: U-Pb age constraints on the timing of Variscan tectonic activity in SW Iberia. *International Journal of Earth Sciences*, 104, 1167-1183.
- Pereira, M.F., Gama, C., Chichorro, M., Silva, J.B., Gutiérrez-Alonso, G., Hofmann, M., Linnemann, U., Gärtner, A., 2016. Evidence for multicycle sedimentation and provenance constraints from detrital zircon U-Pb ages: Triassic strata of the Lusitanian basin (western Iberia). *Tectonophysics*, 681, 318-331.
- Pereira, M.F., Gama, C., Rodríguez, C., 2017a. Coeval interaction between magmas of contrasting composition (Late Carboniferous-Early Permian Santa Eulália—Monforte massif, Ossa-Morena zone): Field relationships and geochronological constraints. *Geologica Acta*, 15(4), 409-428.
- Pereira, M.F., Gutierrez-Alonso, G., Murphy, J.B., Drost, K., Gama, C., Silva, J.B., 2017b. Birth and demise of the Rheic Ocean magmatic arc(s): Combined U-Pb and Hf isotope analyses in detrital zircon from SW Iberia siliciclastic strata. *Lithos*, 278-281, 383-399.
- Pereira, M.F., Gama, C., Dias da Silva, I., Fuenlabrada, J.M., Silva, J.B., Medina, J., 2020. Isotope geochemistry evidence for Laurussian-type sources of South Portuguese Zone Carboniferous turbidites (Variscan Orogeny). In: Murphy, J.B., Strachan, R.A., Quesada, C. (eds.). *Pannotia to Pangaea: Neoproterozoic and Paleozoic Orogenic Cycles in the Circum-Atlantic Region*. London, Geological Society, 503 (Special Publications). DOI: <https://doi.org/10.1144/SP503-2019-163>
- Pimentel, N., Pena dos Reis, R., 2016. Petroleum systems of the West Iberian margin: a review of the Lusitanian basin and the deep offshore Peniche basin. *Journal of Petroleum Geology*, 39(3), 305-326.
- Priem, H.N.A., Boelrijk, N.A.I.M., Verschure, R.H., Hebeda, E.H., 1965. Isotopic ages of two granites on the Iberian continental margin: the Traba granite (Spain) and the Berlenga granite (Portugal). *Geologie en Mijnbouw*, 44, 353-354.
- Puelles, P., Gil Ibarguchi, J.I., García de Madinabeitia, S., Sarrionandia, E., Carracedo-Sánchez, M., Fernández-Armas, S., 2019. Granulite-facies gneisses and meta-igneous xenoliths from the Campo de Calatrava volcanic field (Spain): Implications for the tectonics of the Variscan lower crust. *Lithos*, 342-343, 114-134.
- Quesada, C., Robardet, M., Gabaldon, V., 1990. Ossa-Morena Zone. Stratigraphy. Synorogenic Phase (Upper Devonian–Carboniferous–Lower Permian). In: Dallmeyer, R.D., Martínez, E. (eds.). *Pre-Mesozoic Geology of Iberia*. Berlin-Heidelberg, Springer-Verlag, 273-279.
- Ribeiro, A., Munhá, J., Dias, R., Mateus, A., Pereira, E., Ribeiro, L., Fonseca, P., Araújo, A., Oliveira, T., Romão, J., Chaminé,

- H., Coke, C., Pedro, J., 2007. Geodynamic evolution of the SW Europe variscides. *Tectonics*, 26, doi:10.1029/2006/TC002058.
- Ribeiro, M.L., Reche, J., López-Carmona, A., Aguilar, C., Bento dos Santos, T., Chichorro, M., Dias da Silva, Í., Díez-Montes, A., González-Clavijo, E., Gutiérrez-Alonso, G., Leal, N., Liesa, M., Martínez, E.J., Mateus, A., Mendes, M.H., Moita, P., Pedro, J., Quesada, C., Santos, J.F., Solá, A.R., Valverde-Vaquero, P., 2019. Variscan Metamorphism. In: Quesada, C., Oliveira, J.T. (eds.). *The Geology of Iberia: A Geodynamic Approach*, Volume 2: The Variscan Cycle. Springer International Publishing, 431-495.
- Robardet, M., 2003. The Armorica 'microplate': fact or fiction? Critical review of the concept and contradictory palaeobiogeographical data. *Palaeogeography, Palaeoclimatology, Palaeoecology*, 195(1), 125-148.
- Robardet, M., Gutiérrez-Marco, J.C., 2004. The Ordovician, Silurian and Devonian sedimentary rocks of the Ossa-Morena Zone (SW Iberian Peninsula, Spain). *Journal of Iberian Geology*, 30, 73-92.
- Rocha, R.B., Matioli, E., Duarte, L.V., Pittet, B., Elmi, S., Mouterde, R., Cabral, M.C., Comas-Rengifo, M.J., Gómez, J.J., Goy, A., Hesselbo, S.P., Jenkyns, H.C., Littler, K., Mailliot, S., Veiga de Oliveira, L.C., Osete, M.L., Perilli, N., Pinto, S., Ruget, Ch., Suan, G., 2016. Base of the Toarcian Stage of the Lower Jurassic defined by the Global Boundary Stratotype Section and Point (GSSP) at the Peniche section (Portugal). *Episodes*, 39(3), 460-481.
- Romariz, C., 1963-1964. Notas petrográficas sobre rochas sedimentares portuguesas- a brecha vulcânica da Papôa (Peniche). *Boletim do Museu e Laboratório Mineralógico e Geológico da Faculdade de Ciências de Lisboa*, 10(1), 19-28.
- Rosa, D.R.N., Finch, A.A., Andersen, T., Inverno, C.M.C., 2008. U-Pb geochronology and Hf isotope ratios of magmatic zircon from the Iberian Pyrite Belt. *Mineralogy and Petrology*, 95, 47-69.
- Rosa, A.R., Cachapuz, P., Bento dos Santos, T., Solá, A.R., Romão, J., Valverde-Vaquero, P., Carvalho, D.R., 2019. Correlação petrográfica e geoquímica entre a Brecha Vulcânica da Papôa (Peniche, W Portugal) e o Arquipélago das Berlengas. Extended abstracts, XII Congreso Ibérico de Geoquímica, Portugal, Universidade de Évora, 70-74.
- Rubio-Ordóñez, A., Valverde-Vaquero, P., Corretgé, L.G., Cuesta-Fernández, A., Gallastegui, G., Fernández-González, M., Gerdes, A., 2012. An early Ordovician tonalitic-granodioritic belt along the Schistose-Greywacke Domain of the Central Iberian zone (Iberian Massif, Variscan belt). *Geological Magazine*, 149(5), 927-939.
- Sánchez-García, T., Chichorro, M., Solá, A.R., Álvaro, J.J., Díez-Montes, A., Bellido, F., Ribeiro, M.L., Quesada, C., Lopes, J.C., Dias da Silva, Í., González-Clavijo, E., Gómez Barreiro, J., López-Carmona, A., 2019. The Cambrian-Early Ordovician Rift Stage in the Gondwanan Units of the Iberian Massif. In: Quesada, C., Oliveira, J.T. (eds.). *The Geology of Iberia: A Geodynamic Approach*. Volume 2: The Variscan Cycle. Springer International Publishing, 27-74.
- Shail, R.K., Leveridge, B.E., 2009. The Rheohercynian passive margin of SW England: development, inversion and extensional reactivation. *Comptes Rendus Geoscience*, 341, 140-155.
- Shellnutt, J.G., Owen, J.V., Yeh, M.-W., Dostal, J., Nguyen, D.T., 2018. Long-lived association between Avalonia and the Meguma terrane deduced from zircon geochronology of metasedimentary granulites. *Scientific Reports*, 9, 4065.
- Simons, B., Shail, R.K., Andersen, C.O., 2016. The petrogenesis of the Early Permian Variscan granites of the Cornubian Batholith: Lower plate post-collisional peraluminous magmatism in the Rheohercynian Zone of SW England. *Lithos*, 260, 76-94.
- Stampfli, G.M., Hochard, C., Vêrard, C., Wilhem, C., von Raumer, J., 2013. The formation of Pangea. *Tectonophysics*, 593, 1-19.
- Steiger, R.H., Jager, E., 1977. Subcommission on geochronology; convention on the use of decay constants in geo- and cosmochronology. *Earth Planetary Science Letters*, 36, 359-362.
- Talavera, C., Martínez Poyatos, D., González Lodeiro, E., 2015. SHRIMP U-Pb geochronological constraints on the timing of the intra-Alcudian (Cadomian) angular unconformity in the Central Iberian zone (Iberian Massif, Spain). *International Journal of Earth Sciences*, 104, 1739-1757.
- Tate, M.C., Clarke, D.B., 1995. Petrogenesis and regional tectonic significance of Late Devonian mafic intrusions in the Meguma Zone, Nova Scotia. *Canadian Journal of Earth Sciences*, 32, 1883-1898.
- Terrinha, P., Kullberg, J.C., Neres, M., Alves, T., Ramos, A., Ribeiro, C., Mata, J., Pinheiro, L., Afilhado, A., Matias, L., Luís, J., Muñoz, J.A., Fernández, Ó., 2019. Rifting of the Southwest and West Iberia, 6- Continental Margins. In: Quesada, C., Oliveira, J.T. (eds.). *The Geology of Iberia: A Geodynamic Approach*. Volume 3: The Alpine Cycle. Springer International Publishing, 251-283.
- Valverde-Vaquero, P., Bento dos Santos, T., González Clavijo, E., Díez Montes, A., Ribeiro, M.L., Solá, R., Dias da Silva, Í., 2011. The Berlengas Archipelago granitoids within the frame of the Variscan Orogeny, W Portugal: new data and insights. In: Molina, J.F., Scarrow, J.H., Bea, F., Montero, P. (eds.). VII Hutton Symposium on Granites and Related Rocks, Ávila, 153.
- White, C.E., Barr, S.M., 2012. Meguma Terrane revisited: stratigraphy, metamorphism, paleontology and provenance. *Geoscience Canada*, 39, 8-12.
- White, C.E., Barr, S.M., Linnemann, U., 2018. U-Pb (zircon) ages and provenance of the White Rock Formation of the Rockville Notch Group Meguma terrane, Nova Scotia, Canada: evidence for the "Sardian gap" and West African origin. *Canadian Journal of Earth Sciences*, 55, 589-603.
- Williams, I.S., 1998. U-Th-Pb Geochronology by Ion Microprobe. In: McKibben, M.A., Shanks III, W.C., Ridley, W.I. (eds.). *Applications of microanalytical techniques to understanding mineralizing processes*. *Reviews in Economic Geology*, 7, 1-35.

- Williams, I.S., Hergt, J.M., 2000. U-Pb dating of Tasmanian dolerites: a cautionary tale of SHRIMP analysis of high-U zircon. In: Woodhead, J.D., Hergt, J.M., Noble, W.P. (eds.), *Beyond 2000: New Frontiers in Isotope Geoscience*. Lorne, 2000; Abstracts and Proceedings, 185-188.
- Winter, C., Bretkreu, Ch., Lapp, M., 2008. Textural analysis of a Late Palaeozoic coherent-pyroclastic rhyolitic dyke system near Burkersdorf (Erzgebirge, Saxony, Germany). In: Thomson, K., Petford, N. (eds.). *Structure and Emplacement of High-Level Magmatic Systems*. London, Geological Society, 302 (Special Publications), 199-221.
- Zbyszewski, G., 1959. *Etude Structurale de l'Aire Typhonique de Caldas da Rainha*. Lisboa, Memórias dos Serviços Geológicos de Portugal, 3, 184pp.

**Manuscript received June 2020;  
revision accepted August 2020;  
published Online October 2020.**

# APPENDIX I

**TABLE I.** Zircon U-Pb geochronological data (granitic xenoliths in the Papôa volcanic breccia; Xpp-2, 39°22'27.58"N; 9°22'36.78"W; Xpp-3, 39°22'25.60"N; 9°22'37.70"W)

id	U (ppm)	Th (ppm)	206Pb (ppm)	207Pb (ppm)	206Pb/238U	207Pb/235U	% 206.4	% 208.8	Th/U	common lead uncorrected					common lead uncorrected ages (Ma)							
										isotope ratios	207Pb/206Pb	207Pb/238U	206Pb/238U	207Pb/235U	206Pb/238U	207Pb/235U	206Pb/238U	207Pb/235U	206Pb/238U	207Pb/235U	206Pb/238U	207Pb/235U
Xpp-3-1.1	2419.1	1177.6	101.5	0.2	0.2	0.05	0.00014	0.00001	0.00017	0.04848	0.00037	0.35610	0.00323	0.609	340.5	7.2	305.2	2.3	309.3	2.4	1.4	
Xpp-3-10.1	4572.9	742.0	177.0	0.6	2.1	0.17	0.00032	0.00005	0.05627	0.00012	0.04287	0.00084	0.34545	0.00677	0.222	453.1	8.8	270.6	5.2	301.3	5.1	10.2
Xpp-3-10.2	1649.0	1937.5	63.8	0.9	0.1	1.21	0.00052	0.00022	0.04688	0.00108	0.04688	0.00159	0.35019	0.01421	0.633	485.9	41.2	281.8	9.9	304.9	10.8	7.6
Xpp-3-11.1	2851.2	251.9	107.4	0.1	0.0	1.10	0.00006	0.00001	0.05198	0.00046	0.04667	0.00384	0.34585	0.00384	0.400	284.0	20.0	294.0	1.8	293.8	2.9	0.0
Xpp-3-12.1	1056.9	1278.3	42.8	0.4	-0.1	1.24	0.00024	0.00005	0.05083	0.00063	0.04674	0.00139	0.32763	0.01036	0.676	233.3	23.6	294.5	8.5	287.8	8.5	-2.4
Xpp-3-13.1	1083.1	281.6	117.1	1.1	1.6	0.27	0.00059	0.00009	0.05634	0.00044	0.04652	0.00026	0.34585	0.00360	0.405	465.7	17.2	280.8	1.6	301.6	2.7	6.8
Xpp-3-14.1	3238.4	249.3	129.1	0.1	0.0	0.08	0.00004	0.00003	0.05164	0.00034	0.04639	0.00043	0.32806	0.00396	0.568	269.5	15.2	286.2	2.7	288.1	3.1	0.6
Xpp-3-15.1	2279.6	238.5	92.6	0.5	0.9	0.11	0.00030	0.00006	0.05620	0.00062	0.04693	0.00056	0.36386	0.00608	0.518	460.3	24.4	295.6	3.4	314.9	4.5	6.2
Xpp-3-16.1	738.3	224.1	29.9	0.8	-0.4	0.31	0.00043	0.00006	0.05447	0.00063	0.04672	0.00053	0.35088	0.00532	0.525	390.7	21.6	294.3	3.2	305.4	4.0	3.6
Xpp-3-17.1	1163.4	256.4	45.4	0.6	-1.2	0.23	0.00034	0.00003	0.05411	0.00043	0.04508	0.00034	0.33980	0.00380	0.478	375.7	17.0	284.2	2.1	294.4	2.9	3.4
Xpp-3-18.1	1661.8	1024.9	85.3	26.0	19.6	0.63	0.01431	0.00018	0.24600	0.00462	0.05931	0.00147	0.21183	0.00296	0.570	3159.3	29.4	371.4	6.9	1119.5	21.4	66.8
Xpp-3-19.1	87.0	333.7	333.7	0.3	0.1	0.05	0.00014	0.00004	0.05235	0.00016	0.04614	0.00017	0.33303	0.00200	0.448	300.5	6.8	290.8	1.1	291.9	1.5	0.4
Xpp-3-2.1	7847.0	429.7	333.7	0.3	0.4	0.08	0.00014	0.00001	0.05248	0.00031	0.04988	0.00024	0.36432	0.00952	0.778	381.9	13.0	276.8	7.6	315.4	7.1	12.2
Xpp-3-2.2	1897.8	222.0	80.0	0.4	0.1	0.12	0.00020	0.00000	0.05240	0.00057	0.04871	0.00045	0.35193	0.00851	0.451	302.9	24.8	306.6	2.8	306.2	3.9	-0.2
Xpp-3-20.1	4051.2	146.1	166.4	0.2	0.1	0.04	0.00012	0.00002	0.05260	0.00061	0.04697	0.00095	0.34536	0.00809	0.635	320.1	26.2	289.7	5.8	301.2	6.1	3.8
Xpp-3-3.1	2861.2	232.2	108.1	0.9	0.7	0.09	0.00052	0.00012	0.05772	0.00088	0.04678	0.00227	0.37353	0.00623	0.251	519.3	33.0	284.7	1.7	322.3	4.7	8.6
Xpp-3-4.1	2892.6	261.4	107.5	0.2	0.3	0.10	0.00010	0.00000	0.05488	0.00015	0.04693	0.00073	0.35383	0.00548	0.694	306.3	6.6	289.5	4.5	292.3	4.1	1.0
Xpp-3-5.1	2612.4	223.7	108.2	0.3	0.2	0.09	0.00017	0.00004	0.05411	0.00045	0.04773	0.00063	0.35032	0.00564	0.594	333.5	19.0	300.6	3.9	305.0	4.3	1.4
Xpp-3-6.1	2337.8	447.7	92.9	0.7	-1.1	0.20	0.00041	0.00005	0.05895	0.00064	0.04692	0.00033	0.36506	0.00495	0.372	489.5	24.4	289.4	2.0	312.6	3.7	7.4
Xpp-3-7.1	2005.9	130.4	83.5	0.2	0.1	0.07	0.00011	0.00003	0.05302	0.00046	0.04808	0.00070	0.35148	0.00393	0.628	329.5	19.4	302.7	4.3	305.8	4.5	1.0
Xpp-3-8.1	2615.2	358.8	103.5	0.4	0.6	0.14	0.00024	0.00000	0.05435	0.00024	0.04562	0.00046	0.34285	0.00393	0.628	385.5	9.8	287.6	2.8	299.2	3.0	3.8
Xpp-2-1.1	313.2	303.1	408.1	1.2	1.1	-0.3	0.00690	0.00014	0.05110	0.00097	0.04758	0.00036	0.34841	0.00700	0.271	333.3	40.8	299.7	2.2	303.5	5.3	1.2
Xpp-2-10.1	408.1	249.6	16.7	1.3	0.4	0.63	0.00074	0.00018	0.04739	0.00039	0.04739	0.00039	0.35600	0.00666	0.313	390.9	36.4	298.5	2.4	309.2	5.0	3.4
Xpp-2-11.1	910.3	104.6	35.7	0.7	0.2	0.12	0.00038	0.00013	0.05709	0.00044	0.04635	0.00019	0.35694	0.00336	0.312	495.1	16.8	285.9	1.2	309.9	2.5	7.8
Xpp-2-12.1	355.9	49.4	14.6	0.0	0.1	0.14	0.00001	0.00002	0.05000	0.00029	0.04731	0.00032	0.33267	0.00318	0.509	240.7	13.2	298.0	2.0	291.6	2.4	-2.2
Xpp-2-13.1	202.1	142.4	8.4	0.8	0.2	0.72	0.00044	0.00023	0.05506	0.00078	0.04802	0.00107	0.36456	0.00968	0.603	414.7	31.2	302.4	6.6	315.6	7.2	4.2
Xpp-2-14.1	206.7	217.9	8.5	0.4	0.2	1.06	0.00025	0.00063	0.05348	0.00108	0.04773	0.00038	0.35191	0.00774	0.281	349.1	45.0	300.6	2.4	306.2	5.9	1.8
Xpp-2-15.1	961.8	61.3	38.2	1.2	1.1	0.07	0.00065	0.00015	0.06250	0.00064	0.04685	0.00046	0.35607	0.00587	0.491	691.1	21.8	289.0	2.9	338.1	4.3	14.6
Xpp-2-16.1	1133.2	92.2	44.1	0.4	0.4	0.08	0.00020	0.00006	0.05410	0.00050	0.04500	0.00052	0.33566	0.00511	0.548	375.3	20.4	283.7	3.2	293.9	3.9	3.4
Xpp-2-17.1	1968.8	63.0	74.9	1.4	1.1	0.03	0.00078	0.00007	0.06233	0.00034	0.04988	0.00078	0.37789	0.00715	0.676	685.5	11.6	277.5	4.9	325.6	5.3	14.8
Xpp-2-18.1	836.0	91.4	32.5	0.3	0.5	0.11	0.00015	0.00008	0.05364	0.00064	0.04490	0.00063	0.33210	0.00622	0.536	356.1	26.8	283.1	3.8	291.2	4.8	2.8
Xpp-2-19.1	544.0	46.4	22.0	0.7	0.5	0.09	0.00038	0.00017	0.05419	0.00071	0.04668	0.00052	0.34881	0.00615	0.437	379.1	29.2	284.1	3.2	303.8	4.6	3.2
Xpp-2-20.1	666.6	95.1	27.1	0.4	0.3	0.15	0.00022	0.00013	0.05447	0.00016	0.04704	0.00036	0.33383	0.00306	0.603	262.1	8.0	286.3	2.2	292.5	2.3	-1.2
Xpp-2-21.1	316.3	95.6	13.3	1.1	0.3	0.31	0.00059	0.00023	0.05376	0.00092	0.04645	0.00030	0.35915	0.00665	0.244	361.1	38.0	305.0	1.9	311.6	5.0	2.2
Xpp-2-21.1	1027.5	1488.0	38.6	0.6	-0.3	1.49	0.00033	0.00008	0.05469	0.00207	0.04336	0.00282	0.32569	0.02465	0.622	399.7	82.6	273.6	17.4	287.3	19.1	4.8
Xpp-2-22.1	477.6	449.5	18.8	1.6	1.5	0.97	0.00040	0.00002	0.05749	0.00032	0.04642	0.00075	0.35988	0.00660	0.542	696.5	29.4	286.4	4.7	336.1	4.9	7.2
Xpp-2-3.1	775.6	1127.4	33.3	0.7	52.0	1.49	0.00040	0.00002	0.05749	0.00032	0.04642	0.00075	0.35988	0.00660	0.542	696.5	29.4	286.4	4.7	336.1	4.9	7.2
Xpp-2-4.1	1218.3	102.4	47.2	0.2	-0.1	0.09	0.00010	0.00007	0.05575	0.00045	0.04476	0.00043	0.33171	0.00439	0.523	360.7	18.8	282.2	2.6	290.9	3.4	3.0
Xpp-2-5.1	1302.2	47.8	64.5	2.1	0.1	0.04	0.00015	0.00025	0.05272	0.00022	0.05722	0.00038	0.41615	0.02613	0.717	317.9	9.2	386.7	21.9	353.3	18.9	-1.6
Xpp-2-6.1	1022.3	94.8	40.9	0.4	0.1	0.10	0.00020	0.00000	0.05297	0.00036	0.04620	0.00030	0.33746	0.00338	0.466	327.7	15.2	291.2	1.9	295.2	2.5	1.4
Xpp-2-7.1	1553.5	34.2	58.7	0.6	0.4	0.02	0.00035	0.00001	0.05531	0.00028	0.04363	0.00064	0.33277	0.00533	0.663	424.9	11.4	275.3	4.0	291.7	4.1	5.6
Xpp-2-8.1	3995.6	163.6	150.6	0.1	0.1	0.04	0.00007	0.00002	0.05367	0.00035	0.04225	0.00058	0.32224	0.00491	0.647	357.1	14.6	266.7	3.5	283.6	3.8	6.0
Xpp-2-9.1	1428.4	41.9	54.4	0.5	0.3	0.03	0.00027	0.00006	0.05281	0.00060	0.04403	0.00061	0.32063	0.00583	0.545	320.7	25.6	277.8	3.8	282.4	4.5	1.6

SHRIMP-TOOLs data processing; IBERINSIMS laboratory, University of Granada, Spain  
 Errors are at 1-sigma level  
 Point-to point errors, calculated on replicates of the TEMORA standard at 95% confidence interval, are: 0.34 % for 206Pb/238U, and 0.39 % for 207Pb/206Pb

TABLE I. Continued

id	204-corrected isotope ratios		204-corrected ages (Ma)		207Pb/235U		206Pb/238U		207Pb/235U		206Pb/238U		207Pb/235U		206Pb/238U		terr	% discord.
	207Pb/206Pb	terr	207Pb/206Pb	terr	207Pb/235U	terr	206Pb/238U	terr	207Pb/235U	terr	206Pb/238U	terr	207Pb/235U	terr	206Pb/238U	terr		
Xpp-3-1.1	0.05125	0.00027	0.04836	0.00037	0.34173	0.00342	0.01405	0.00079	252.3	122.2	304.4	2.3	286.5	2.6	287.4	2.6	-2.0	
Xpp-3-10.1	0.05127	0.00086	0.04262	0.00084	0.30126	0.00788	0.02116	0.00053	253.1	182.2	269.0	5.2	267.4	6.2	267.4	6.2	-0.6	
Xpp-3-10.2	0.04923	0.00363	0.04266	0.00159	0.30042	0.02485	0.01336	0.00046	158.9	163.8	279.2	9.8	266.7	19.4	266.7	19.4	-4.6	
Xpp-3-11.1	0.05106	0.00047	0.04661	0.00030	0.32820	0.00386	0.01400	0.00022	243.7	21.0	293.7	1.8	288.2	3.0	288.2	3.0	-2.0	
Xpp-3-12.1	0.04733	0.00101	0.04654	0.00138	0.30373	0.01115	0.01425	0.00029	65.9	50.0	293.3	8.6	269.3	8.7	269.3	8.7	-8.0	
Xpp-3-13.1	0.04759	0.00153	0.04404	0.00027	0.28900	0.00954	0.01558	0.00076	79.1	74.8	277.8	1.6	281.5	7.6	277.8	7.6	-1.6	
Xpp-3-14.1	0.05103	0.00053	0.04536	0.00043	0.31954	0.00467	0.01375	0.00063	244.9	24.0	286.0	2.7	287.8	3.6	287.8	3.6	-1.6	
Xpp-3-15.1	0.05186	0.00108	0.04668	0.00337	0.33378	0.00813	0.01748	0.00096	279.5	47.0	294.1	3.5	292.4	6.2	292.4	6.2	-0.6	
Xpp-3-16.1	0.04806	0.00107	0.04634	0.00062	0.30709	0.00771	0.01098	0.00040	102.1	51.8	292.0	3.1	271.9	6.0	271.9	6.0	-7.4	
Xpp-3-17.1	0.04909	0.00068	0.04480	0.00034	0.30317	0.00491	0.00688	0.00049	151.9	32.2	282.5	2.1	268.9	3.9	268.9	3.9	-5.0	
Xpp-3-18.1	0.02998	0.00734	0.04373	0.00110	0.18076	0.04451	0.00186	0.00099	0.0	98.9	275.9	6.8	188.0	39.0	188.0	39.0	-63.6	
Xpp-3-19.1	0.05024	0.00070	0.04602	0.00018	0.31881	0.00474	0.01171	0.00166	206.3	31.8	290.0	1.0	281.0	3.7	281.0	3.7	-3.2	
Xpp-3-2.1	0.05174	0.00037	0.04376	0.00124	0.31219	0.00917	0.01589	0.00040	273.9	16.2	276.1	7.6	275.9	7.1	275.9	7.1	0.0	
Xpp-3-2.2	0.04946	0.00058	0.04653	0.00045	0.33096	0.00507	0.01335	0.00032	169.7	27.0	305.5	2.8	290.3	3.9	290.3	3.9	-5.2	
Xpp-3-20.1	0.05110	0.00071	0.04587	0.00095	0.32323	0.00813	0.01183	0.00108	245.5	31.6	289.1	5.8	284.4	6.3	284.4	6.3	-1.6	
Xpp-3-3.1	0.05003	0.00206	0.04633	0.00029	0.31958	0.01333	0.01153	0.00261	196.3	92.8	292.0	1.8	280.6	10.3	280.6	10.3	-3.6	
Xpp-3-4.1	0.05050	0.00227	0.04577	0.00083	0.31866	0.01548	0.00967	0.00073	217.9	100.8	288.5	5.1	281.9	12.0	281.9	12.0	-2.8	
Xpp-3-5.1	0.05107	0.00016	0.04585	0.00073	0.32286	0.00534	0.01565	0.00024	244.1	7.2	289.0	4.5	284.1	4.1	284.1	4.1	-1.8	
Xpp-3-6.1	0.05067	0.00081	0.04759	0.00063	0.33244	0.00700	0.01326	0.00090	225.7	36.4	299.7	3.9	291.4	5.3	291.4	5.3	-2.8	
Xpp-3-7.1	0.05099	0.00105	0.04558	0.00033	0.32043	0.00707	0.00579	0.00056	240.3	46.6	287.3	2.0	282.2	5.4	282.2	5.4	-1.8	
Xpp-3-8.1	0.05133	0.00061	0.04798	0.00070	0.33960	0.00649	0.01373	0.00075	255.9	27.0	302.1	4.3	296.9	5.0	296.9	5.0	-1.8	
Xpp-3-9.1	0.05087	0.00024	0.04542	0.00045	0.31862	0.00371	0.01567	0.00003	235.1	10.8	286.4	2.8	280.8	2.8	280.8	2.8	-2.0	
Xpp-2-1.1	0.04426	0.00238	0.04706	0.00338	0.28719	0.01567	0.01357	0.00029	0.0	30.9	296.5	2.3	256.3	12.4	256.3	12.4	-15.6	
Xpp-2-10.1	0.04352	0.00297	0.04675	0.00041	0.28058	0.01931	0.01334	0.00058	0.0	23.1	294.6	2.6	251.1	15.4	251.1	15.4	-17.4	
Xpp-2-11.1	0.05152	0.00202	0.04503	0.00021	0.31890	0.01270	0.01039	0.00184	264.3	87.8	283.9	1.3	281.8	9.8	281.8	9.8	-0.8	
Xpp-2-12.1	0.05080	0.00039	0.04730	0.00032	0.33130	0.00358	0.01545	0.00083	231.9	17.4	297.9	2.0	290.6	2.8	290.6	2.8	-2.6	
Xpp-2-13.1	0.04858	0.00370	0.04763	0.00108	0.31908	0.02538	0.01417	0.00069	127.7	170.2	300.0	6.7	281.2	19.7	281.2	19.7	-6.6	
Xpp-2-14.1	0.04986	0.00998	0.04751	0.00667	0.32667	0.06557	0.01469	0.01008	188.7	409.4	299.2	4.1	287.0	51.5	287.0	51.5	-4.2	
Xpp-2-15.1	0.05296	0.00245	0.04530	0.00048	0.33080	0.01576	0.01335	0.00404	327.1	101.8	285.6	2.9	290.2	12.1	290.2	12.1	1.6	
Xpp-2-16.1	0.05112	0.00100	0.04483	0.00052	0.31601	0.00730	0.01399	0.00116	246.5	44.6	282.7	3.2	278.8	5.6	278.8	5.6	-1.4	
Xpp-2-17.1	0.05084	0.00120	0.04335	0.00077	0.30387	0.00904	0.00515	0.00377	233.5	53.4	273.6	4.8	269.4	7.0	269.4	7.0	-1.6	
Xpp-2-18.1	0.05136	0.00137	0.04477	0.00063	0.31709	0.00965	0.01565	0.00119	257.3	60.2	282.4	3.9	279.7	7.5	279.7	7.5	-1.0	
Xpp-2-19.1	0.04864	0.00279	0.04636	0.00054	0.31093	0.01823	0.01222	0.00338	130.7	129.6	292.1	3.3	274.9	14.2	274.9	14.2	-6.2	
Xpp-2-2.1	0.04824	0.00209	0.04685	0.00038	0.31159	0.01377	0.01427	0.00170	111.1	99.0	295.1	2.3	275.4	10.7	275.4	10.7	-7.2	
Xpp-2-20.1	0.04498	0.00381	0.04793	0.00037	0.29726	0.02528	0.01271	0.00158	0.0	137.9	301.8	2.3	264.3	20.0	264.3	20.0	-14.2	
Xpp-2-21.1	0.04981	0.00244	0.04310	0.00281	0.29601	0.02413	0.01311	0.00028	186.3	110.0	272.0	17.4	263.3	19.1	263.3	19.1	-3.4	
Xpp-2-22.1	0.04938	0.00261	0.04467	0.00075	0.30417	0.01688	0.01389	0.00031	166.1	118.8	281.7	4.6	269.7	13.3	269.7	13.3	-4.4	
Xpp-2-3.1	0.05159	0.00048	0.04930	0.00076	0.35068	0.00643	0.04324	0.00032	267.1	21.2	310.2	4.6	305.2	4.8	305.2	4.8	-1.6	
Xpp-2-4.1	0.05229	0.00114	0.04467	0.00043	0.32206	0.00775	0.01139	0.00133	297.9	49.0	281.7	2.6	283.5	6.0	283.5	6.0	0.6	
Xpp-2-5.1	0.05555	0.00397	0.05602	0.00351	0.27459	0.03516	-0.04417	-0.01438	0.0	98.9	351.4	21.5	246.4	28.4	246.4	28.4	-42.6	
Xpp-2-6.1	0.05001	0.00036	0.04603	0.00030	0.31741	0.00329	0.01177	0.00029	195.5	16.8	290.1	1.8	279.9	2.5	279.9	2.5	-3.6	
Xpp-2-7.1	0.05022	0.00033	0.04336	0.00064	0.30019	0.00498	0.00444	0.00130	205.1	15.2	273.6	4.0	266.5	3.8	266.5	3.8	-2.6	
Xpp-2-8.1	0.05261	0.00049	0.04219	0.00058	0.30603	0.00517	0.01343	0.00094	311.9	21.0	266.4	3.6	271.1	4.0	271.1	4.0	1.8	
Xpp-2-9.1	0.04895	0.00116	0.04382	0.00061	0.29512	0.00817	0.00849	0.00365	140.5	54.8	276.4	3.7	262.6	6.4	262.6	6.4	-5.2	